

1-1-2003

# The role of univariate and multivariate data in the design of advanced operator workstations

Melinda Marie Cerney  
*Iowa State University*

Follow this and additional works at: <https://lib.dr.iastate.edu/rtd>

 Part of the [Mechanical Engineering Commons](#)

## Recommended Citation

Cerney, Melinda Marie, "The role of univariate and multivariate data in the design of advanced operator workstations" (2003).  
*Retrospective Theses and Dissertations*. 17497.  
<https://lib.dr.iastate.edu/rtd/17497>

This Thesis is brought to you for free and open access by the Iowa State University Capstones, Theses and Dissertations at Iowa State University Digital Repository. It has been accepted for inclusion in Retrospective Theses and Dissertations by an authorized administrator of Iowa State University Digital Repository. For more information, please contact [digirep@iastate.edu](mailto:digirep@iastate.edu).

The role of univariate and multivariate data in the design of advanced operator workstations

by

Melinda Marie Cerney

A thesis submitted to the graduate faculty  
in partial fulfillment of the requirements for the degree of  
MASTER OF SCIENCE

Major: Mechanical Engineering

Program of Study Committee:  
Judy M. Vance (Major Professor)  
Dean C. Adams  
James H. Oliver

Iowa State University

Ames, Iowa

2003

Graduate College  
Iowa State University

This is to certify that the master's thesis of  
Melinda Marie Cerney  
has met the requirements of Iowa State University

Signatures have been redacted for privacy

## TABLE OF CONTENTS

LIST OF FIGURES .....	v
LIST OF TABLES.....	vii
ACKNOWLEDGEMENTS.....	viii
CHAPTER 1: INTRODUCTION.....	1
CHAPTER 2: LITERATURE REVIEW.....	3
2.1 Description of the Data.....	3
2.2 The Application of Traditional Anthropometric Data to Design Scenarios.....	7
2.2.1 Percentile Methods.....	7
2.2.2 Regression Analysis.....	8
2.2.3 Principal Components Analysis.....	9
2.3 Univariate and Multivariate Anthropometric Data.....	10
CHAPTER 3: STATISTICAL COMPARISON OF UNIVARIATE AND MULTIVARIATE ANTHROPOMETRIC DATA.....	12
3.1 Introduction and Data Description.....	12
3.2 Analysis I.....	16
3.2.1 Data and Summary Statistics.....	16
3.2.2 Data Set Comparison.....	18
3.2.3 Conclusions.....	28
3.3 Analysis II.....	29
3.3.1 The Data.....	29
3.3.2 Data Set Comparison.....	30
3.3.3 Conclusions.....	36
CHAPTER 4: WORKSTATION DESIGN TOOL.....	39
4.1 Virtual Reality and Visualization.....	39
4.2 Application Implementation.....	42
4.2.1 Processing and Viewing the Data.....	43
4.2.2 Interaction Methods.....	45
4.2.3 Use of Existing CAD Geometry.....	47
4.2.4 Element Selection.....	48
4.2.5 Subject Discrimination: Density Contours.....	49
4.2.6 Posture Data Examination Methods.....	52
4.2.7 Principal Components Analysis.....	54
CHAPTER 5: CONCLUSIONS.....	56
5.1 Conclusions and Discussion.....	56
5.2 Recommendations for Future Work.....	58

APPENDIX.....	60
A. Three-Dimensional Landmark Descriptions.....	60
B. Traditional Distance Descriptions.....	61
REFERENCES .....	64

## LIST OF FIGURES

Figure 1: Traditional anthropometric distance measures for seated posture..	3
Figure 2: CAESAR body scan types.....	6
Figure 3: Traditional anthropometric measurements for seated posture. ....	13
Figure 4: Three-dimensional landmark locations. ....	14
Figure 5: First two principal axes of traditional distance data.....	23
Figure 6: First two principal axes of extracted distance data.....	23
Figure 7: 95 <sup>th</sup> percentile density contour and case selections for traditional distance data set. ....	25
Figure 8: 95 <sup>th</sup> percentile density contour and case selections for extracted distance data set. ....	26
Figure 10: Correlation plot of the results of the Mantel test including the extracted distance data and the traditional distance data sets. ....	28
Figure 11: First two principal axes of 3D landmark data. ....	33
Figure 12: First two principal axes of extracted distance data.....	33
Figure 13: The first three principal axes of the 3D landmark data. ....	35
Figure 14: Correlation results from the Mantel test involving the extracted distance data and the 3D landmark data sets. ....	36
Figure 15: Inspection of pedal reach for a subject in a John Deere Cab using the immersive virtual environment.....	40
Figure 16: The C4 and the C6 virtual environments.....	42
Figure 17: Relationship between seat index point, seat origin, and the CAESAR butt block landmark.....	43
Figure 18: Motion paths and body scan for a subject displayed in the C6. ....	45
Figure 19: The RF Wand. ....	45
Figure 20: Menu interaction in the virtual environment.....	46

Figure 21: Commands for the Main, View, Selection, and Manipulation menus. ....	46
Figure 22: Landmarks for selected subjects displayed. ....	49
Figure 23: 95th percentile density contours for individual landmarks. ....	50
Figure 24: LineMen. ....	53
Figure 25: Two subjects selected from the principal components plot. ....	55
Figure 26: A possible truss configuration for the analysis based on 10 landmarks.....	57

## LIST OF TABLES

Table 1: Measurement methods for inter-point landmark distance calculation.....	17
Table 2: Mean and standard deviation values for measurements from traditional distance and extracted distance data sets. ....	17
Table 3: Correlation table for measurements, showing values for both traditional and extracted data sets .....	19
Table 4: Coefficients for the principal components from traditional distance data.....	21
Table 5: Coefficients for the principal components from extracted distance data. ....	21

## ACKNOWLEDGEMENTS

I would like to express my gratitude to Dr. Judy Vance for her guidance and encouragement on this work and throughout my undergraduate and graduate studies.

I would also like to recognize Dr. Dean Adams and Dr. Jim Oliver for serving on my committee. Additional thanks go to Dr. Adams specifically for his animated introduction to the field of morphometrics and his invaluable suggestions.

I am grateful to Jerry Duncan and Deere & Co. for their help and support.

Finally, I would like to express my deep appreciation to my parents, who have always been certain that I would succeed, even when I was unsure.

## CHAPTER 1: INTRODUCTION

The application of human figure data in workstation design has typically relied on “traditional” anthropometric data—length, breadth, width, and height values recorded when the subject is positioned in standard, erect anthropometric postures. In spite of the increasing availability of three-dimensional data, many human factors and ergonomics decisions continue to be based upon these univariate anatomical measures through the use of summary statistics such as the 95<sup>th</sup> percentile seated eye height or generalized design cases like the 5<sup>th</sup> percentile female. These methods simplify the representation of a population with a collection of one-dimensional measurements which fail to maintain the form information or homology of the original subjects.

This thesis will explore the use of three-dimensional landmark data as a more complete method of representing the human form, through

- statistical comparison of the characteristics of traditional, univariate anthropometric data to three-dimensional anthropometric data, and
- description of the development of an immersive, virtual reality application used to design operator workstations based on 3D anthropometric data.

Chapter 2 will present a review of the literature, focusing on the current design methodology and the differences between distance-based and three-dimensional descriptive data in anthropometric design. In Chapter 3, traditional distance data, distance data extracted from the 3D data set, and three-dimensional landmark data are compared through an array of statistical and multivariate methods in order to explore whether subjective posturing hinders design methods or enhances them and whether distance data is capable of capturing the subject’s true size and shape for purposes of design. Chapter 4 details an advanced operator

workstation design tool which allows for the use and examination of three-dimensional landmark data, body scans, and motion paths relative to a workstation design in an immersive, virtual reality environment. Finally, Chapter 5 offers a summary of the findings from the previous chapters and delineates some areas of possible future work.

## CHAPTER 2: LITERATURE REVIEW

### 2.1 Description of the Data

Anthropometric data collection traditionally consists of the measurement of the specific surface landmarks which perform at least one of the following functions: identify underlying bony structure, aide in segmentation of the body, produce anatomical reference axis systems for the major body segments, or serve as reference points for the determination of joint centers [1,2]. Traditional anthropometric measurements are taken using anthropometers (distance measuring device), calipers (spreading, sliding, and skinfold), and steel tape measures. During data collection, volunteers are asked to assume stiff, erect postures which help insure repeatability and accuracy in measurement (Figure 1). The result of these surveys is a collection of univariate descriptors of body size in terms of heights, lengths, breadths, depths, girths, weight or mass, skinfold thickness, and surface curvatures for the measured population.

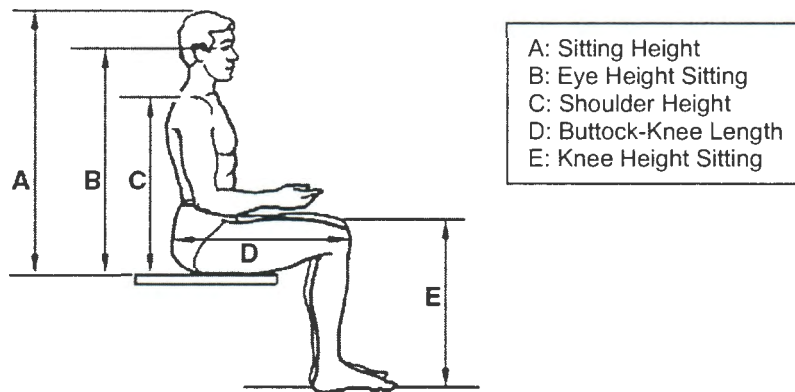


Figure 1: Traditional anthropometric distance measures for seated posture. Image from [3].

Until recently, the most comprehensive anthropometric surveys—and thus the most widely used in making anthropometric design decisions—have been those of military

populations. Anthropometry and body size data was collected from military personnel as early as the Civil War. More focused efforts on the measuring of men and women in the Army Air Forces and the application of this data to engineering design began in 1942 [4]. Today, the most frequently used anthropometric data set is the 1988 Army Anthropometric Survey (ANSUR) of 240 measures for 1,224 men and 2,208 women. Prior to this survey, anthropometric design decisions were based on the 1977 survey of Army women [5], the 1972 survey of Air Force women [6], and the 1967 Air Force male sample [7].

The last comprehensive survey of United States civilian adults was a survey of women conducted by the Department of Agriculture in 1939, which focused on measurements particular to clothing applications [8]. More recently, the Health and Nutritional Examination Studies by the National Center for Health and Statistics collected a handful of measurements in a survey focused primarily on health-related data rather than design data [9], while Stoudt, et al. collected a variety of basic anthropometric measurements in their 1960-1962 survey [10].

The completion of the Civilian American and European Surface Anthropometry Resource (CAESAR) in 2001 provided the design community with a comprehensive set of anthropometric data for approximately 4500 civilian individuals and the first full-body 3-D surface anthropometry survey of the U.S. and Europe. The CAESAR project was carried out by a team from the U.S. Air Force's Computerized Anthropometric Research and Design (CARD) Laboratory, and was funded through support from the Department of Defense, and Society of Automotive Engineers (SAE) partners in automotive, aerospace, heavy equipment, and apparel industries. The survey encompassed volunteers between the ages of 18-65 in the

United States, Italy, and the Netherlands, and made an attempt to include both lightweight and heavyweight subjects [11].

The CAESAR survey collected four types of data:

- 1) demographic information
- 2) univariate measures:
  - forty univariate measures (distance, circumference, skinfold thickness, etc.) taken with traditional tools in standard anthropometric postures (hereafter referred to as *traditional distance measures*)
  - 59 univariate measures extracted from the 3D scan data (*extracted distance measures*)
- 3) complete 3D surface scans in three postures
- 4) 3D coordinates for 73 pre-determined landmarks in each of the three scan postures (*three-dimensional landmark data*).

As previous anthropometric surveys had collected only traditional distance measures and limited demographic information, the CAESAR survey differed dramatically in its inclusion of three-dimensional surface scans and three-dimensional landmark data. In addition, these three-dimensional data were obtained from subjects positioned in non-traditional, relaxed postures, rather than the standard anthropometric postures used in the traditional measurements.

Three-dimensional surface scans were obtained for all participants in each of three postures shown in Figure 2 by scanners which use both lasers and digital imaging to capture color and range data with resolutions to within a few millimeters. Through the use of auto-landmarking software developed for the project, the locations of 73 anatomical landmark locations were derived from these scans and recorded for each subject in all three postures [16].

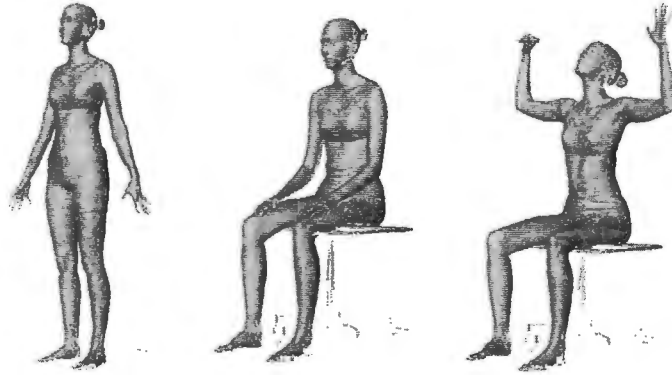


**Figure 2: CAESAR body scan types. From left to right: standing, seated working, and seated coverage postures. Image from [1].**

Traditional anthropometric descriptors were collected during the CAESAR survey in addition to three-dimensional landmark and scan data in order to accommodate traditional design models, allow for comparison with three-dimensional descriptors, and include measurements not easily captured from a surface scan (e.g. weight, mass, skinfold thickness). Some common circumference measures and other distance measures in which the measuring device follows the contours and spans hollows of the body may not be comparable to measures extracted from the scans.

One drawback of using scanning technology to collect surface data is that body surfaces and segments may be obscured from view in the 3D scans, and thus the scanner is unable to collect data for these areas. Typical areas of obscuration include the inner thighs and the area under the arms when standing; between the legs, the back of the thighs, the buttocks, and the lower abdomen when the subject is seated [16].

## 2.2 The Application of Traditional Anthropometric Data to Design Scenarios

### 2.2.1 Percentile Methods

In designing advanced operator workstations so that they can be utilized safely, effectively, and comfortably, it is the task of the designer to accommodate and fit large numbers of an amazingly diverse population. Traditional methods of ergonomic design have relied heavily upon the one-dimensional anthropometric data sets that describe anatomical distance measures. These data sets are most commonly utilized through a “percentile” approach, a method in which designs are specified to accommodate a range of users (e.g., the fifth percentile female through the ninety-fifth percentile male). Percentiles relate the position of an individual value relative to the sample group. The 95<sup>th</sup> percentile stature value, for example, indicates the height at which 95 percent of the measured subjects have smaller values, while the remaining 5 percent are taller.

Digital human modeling tools and individual industrial users have made use of the percentile approach in the form of manikins created to represent the fifth, fiftieth, or ninety-fifth percentile dimensions for each gender in an attempt to produce two or three-dimensional templates by which a design’s accommodation may be judged. Jack [12], SAFEWORK Pro [13], Anthropos, Ramsis [14], and DI-Guy [15] are examples of digital human modeling tools commonly used in ergonomic design.

There are, however, several inherent problems with the percentile method. Percentiles are specific to the population for which they were calculated, and are relevant to only the single dimension they describe. As mentioned above, the most widely used data on body sizes of North American adults was derived from measurements on US Army personnel

recorded in 1988. Military personnel are required to meet strict fitness and health criteria and tend to be younger than the general civilian population, however, making direct comparison to civilian populations extremely difficult [16]. Gordon et al. [17] concluded that this data presents a military bias, and is not directly applicable to designs for civilians. Robinette and McConville [18] demonstrated that percentiles are not additive, and that using percentiles to represent multiple body dimensions leads to gross inaccuracy and over-designing or under-designing for the desired population. Additionally, simultaneous consideration of key measurement values may result in designs which accommodate less of the population than the percentile method implies. Bittner [19] demonstrated that placing 95th and 5th percentile limits on each of 13 dimensions in a multivariate design would exclude 52 percent of the population, instead of the 10 percent implied by the percentile limits.

### 2.2.2 Regression Analysis

Alternate methods of utilizing traditional anthropometric data have been proposed in order to more effectively characterize body size. The first of these is regression analysis, a method of particular use in the construction of crash test dummies. Regression analysis is a mathematical technique that is used to determine the values of parameters for a function that cause the function to best fit a set of given data observations by minimizing the sum of the squared residual values for the observation set [20]. Regression estimates the coefficients of the linear equation involving one or more independent variables which best predicts the value of the dependent variable. The most common use of this method in anthropometric design is to predict body size dimensions for an individual, given that individual's stature and/or weight.

Unlike the percentile method, regression equations provide additive values which can be assembled to match the dimensions of a real individual. For a regression analysis of a standing individual, for example, the toe to knee, knee to waist, and waist to top-of-head measurements would sum to the total height or stature. In the case of a measurement variable which is not highly correlated with the independent variable, however, the prediction based on the regression analysis will be closer to the average for the sample population than the actual value. In addition, regression analysis results are not always indicative of the tendency of human subjects to vary in their *combination* of dimensions. Not present in the regression analysis results are the long-limbed and short torso group of individuals, those with small head dimensions but large body measurements, or other typical body segment combination types [21].

### 2.2.3 Principal Components Analysis

A more effective and more common method of utilizing traditional univariate anthropometric data is the application of principal components analysis and density contours to a set of variables intrinsic to a particular design. Introduced to the ergonomic design community by Bittner et al [22] in 1986 and since refined and simplified, these multivariate methods enable designers to select a desired population to be accommodated in such a way that size differences as well as body proportion variability are taken into account. Additionally, this method allows designers to generate a set number of cases, or manikins which define the extents of their desired design population [11]. These methods will be presented in more detail in Chapter 4.

## 2.3 Univariate and Multivariate Anthropometric Data

As anthropometric measuring techniques have expanded to include the possibility of three-dimensional landmark data, the application of this new, higher-order data is likely to be the most effective method of ensuring accurate designs. Traditional anthropometric databases are a collection of univariate body size descriptors that lack a unifying origin to which they may be related in a three-dimensional space. Additionally, it is not possible to correctly derive the original shape of the individual from these distance measurements [23]. Translation of the anthropometric data into a digital human model introduces inaccuracies, as the digital model requires three-dimensional internal and contour measurements as well as defined geometric relationships not available in traditional collection methods [24].

The landmarks obtained in the CAESAR survey and the scans from which they were extracted represent a significant break from the traditional methods of anthropometric design. By collecting anatomical landmark locations rather than traditional distance measurements, relationships among landmarks are preserved and an individual's homology maintained.

Chapter 3 will compare this new, three-dimensional data to the traditional, univariate distance data through a series of statistical analyses. First, the traditional distance data and distance data extracted from the 3D surface scans of subjects in a seated posture will be used to explore the effects of both posturing and measurement differences. Next, the extracted distance data will be compared to the three-dimensional landmark data. In this analysis, the ability of univariate measures to represent the human form in terms of size and shape characteristics will be evaluated and compared to the description of form afforded by the 3D landmarks.

Chapter 4 presents a virtual reality tool which makes use of the three-dimensional anthropometric data in a three-dimensional space. This advanced operator workstation design tool offers designers the ability to examine the landmark and scan data in an immersive setting, allowing for to-scale interactions and exploration of the data in relation to existing CAD geometry. The chapter will highlight filtering and selection methods for the data and demonstrate how the landmark relationships specified by 3D data can be utilized in an immersive, 3D design space.

## CHAPTER 3: STATISTICAL COMPARISON OF UNIVARIATE AND MULTIVARIATE ANTHROPOMETRIC DATA

### 3.1 Introduction and Data Description

The three-dimensional landmark data collected during the CAESAR survey provides designers with a more accurate description of the body structure and homology of the civilian population than do traditional, anthropometric distance measures. With increased accuracy, however, comes an increase in the amount of information which must be examined in order to make effective design decisions. In the case of the CAESAR data, displaying 73 surface landmarks for 4500 individuals—the total subject set—would be intensely demanding for the display device and overwhelming for the designer.

This chapter will focus on the distance and landmark data for 2703 North American subjects from the CAESAR survey as the data pertains to the design of a seated workstation. Traditional distance measures, distance measures extracted from the three-dimensional landmark data, and the landmark data itself will be compared through the exploration of three design questions:

- the effect of erect versus comfortable posturing on design decisions (*Analysis I*)
- the ability of distance data extracted from 3D landmark data to be used in traditional anthropometric analyses (*Analysis I*)
- the degree of similarity between the design information provided by univariate descriptors (the extracted distance data) and three-dimensional landmark coordinates (*Analysis II*)

All measurements are from the CAESAR database. The traditional and extracted distance measures are univariate descriptors collected in the traditional methods or extracted

from the 3D scan data respectively. The landmark data is xyz position data extracted from the 3D body scans.

As described in [11] and [21], the method of workstation design using multivariate anthropometric data begins with the selection of dimensions or landmark descriptions crucial to the design. In the case of cockpit design—the design scenario for which these methods were first implemented—the most crucial anthropometric dimensions describing body size variability are sitting height, eye height sitting, acromion height sitting, thumbtip reach, buttock-knee length, and knee height sitting. For designs which allow adjustability in order to maintain comfortable and safe body clearance and visibility levels, these are the dimensions which may be used to ensure accommodation (Figure 3). Descriptions of these distance measures appear in the Appendix.

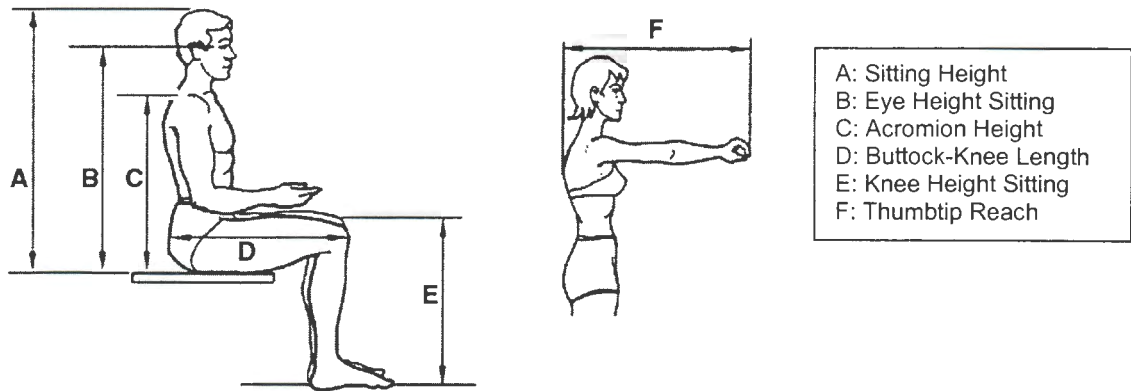


**Figure 3: Traditional anthropometric measurements for seated posture. Image from [3].**

In order to compare the three-dimensional data directly to distance data, the following corresponding landmark locations were used (Figure 4): sellion, left and right acromion, left and right dactylion (tip of the middle finger), left and right femoral epicondyle lateral (outer knee), left and right digit II (tip of the second toe), and the functional butt block. Descriptions of these landmarks appear in the Appendix.

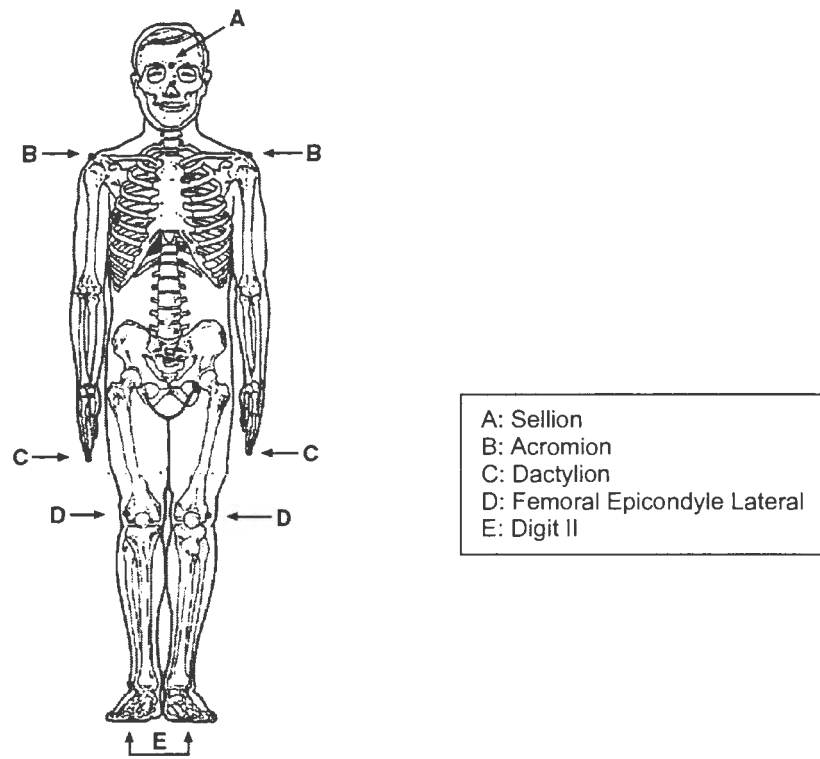


Figure 4: Three-dimensional landmark locations. Image from [1].

These landmarks were selected as they most closely identify the measurement locations for the traditional distance measures, and thus quantify representation of the space occupied by each subject in the most similar way. It is important to note that the *functional* butt block landmark location was used, instead of the measured butt block landmark location. The measured butt block indicates the midpoint of the back side of a wooden block placed behind the seated subject on the flat seat surface. Calculated from the measured butt block, the functional butt block point describes the intersection of the subject's buttocks with the seat platform, and thus is used to identify the top of the seat platform and the rearmost point of the buttocks.

The coordinate values for the extracted distance analysis and the three-dimensional landmark analysis were taken directly from the seated, full body scan data. While this posture is ideal for seated design analysis, the placement of the hands (comfortably resting on the thighs) and the bent posturing of the arms make direct comparison with the standard distance measurements describing arm length difficult. As the thumb-tip reach value was included in the analysis as a gauge of the subject's ability to contact a target, using landmark coordinates for the elbow and hand in order to describe total arm length would have introduced unnecessary description of forearm, elbow, and upper arm posturing into the data set. In order to afford the most accurate comparison between the traditional distance data, a set of landmarks describing straight-arm posturing were required.

In order to improve the similarity of the measurement descriptors, the vector distance from the acromion to the dactylion was extracted from the standing posture body scan (in which each subject's arms are extended at their sides). This relationship was applied to the acromion positions in the seated scan for each subject, effectively placing the hands abducted slightly away from the seated body. In this position, the acromion and middle finger landmarks could be used to calculate an equivalent reach distance (fingertip reach) or used in the 3D landmark analysis to incorporate arm length into the design. This transformation was applied prior to standardization of the landmarks to the seat. No rotations about the acromion point were performed, as the goal was to remain as true to the measured values as possible.

All landmark data was standardized for position and orientation prior to analysis in order to eliminate any noise due to differences in positioning during data collection. All seated subject data was transformed to the same seated reference such that each subject's butt block location was positioned relative to the seat origin, as seen in Figure 16.

The basic data set included all North American CAESAR subjects. Seventy-two of the subjects were removed prior to the analysis as they were missing a value for one of the primary landmark points, leaving 2307 subjects with complete data.

In the first analysis, the effects of posturing are examined by comparing the results of a design solution using distance measures in the anthropometric posture (traditional) with distance measures collected from subjects comfortably postured (extracted). In the second analysis, the effects of using higher-dimensional data are explored by examining the results of using 3D landmark data rather than distance data in an accommodation model. All calculations were performed in JMP [25] and NTSYS-pc software [26].

## 3.2 Analysis I

### 3.2.1 Data and Summary Statistics

In order to compare the comfortable seated posture with the traditional anthropometric posturing, inter-point landmark distance measures were calculated from the seated landmark data for each subject. As direct correspondence between measurement and landmark points was not always possible, the landmarks which most closely described the distance measurement were used. (The seated height distance commonly used in cockpit design was left out of the comparison analysis as no landmark depicting the top of the head was collected in the CAESAR survey, and the seated height and seated eye height values are highly correlated,  $r=0.98$ .) The methods used to calculate the inter-landmark distances are listed in Table 1. Euclidian distance refers to straight-line, three-dimensional distance,  $d$ ,

$$d = \sqrt{(x_1 - x_2)^2 + (y_1 - y_2)^2 + (z_1 - z_2)^2} \quad (1)$$

in which  $(x_1, y_1, z_1)$  is the first landmark point and  $(x_2, y_2, z_2)$  is the second landmark point. Z-distance is the vector distance calculated only in the z-axis direction (the direction from the ground to the top of the head), and is the difference between the z coordinate values for each landmark.

**Table 1: Measurement methods for inter-point landmark distance calculation.**

Distance Measure	Landmarks Used	Calculation Method
Acromion height	acromion, functional butt block	z-distance
buttock-knee length	functional butt block, femoral epicondyle lateral	Euclidian distance
eye height sitting	sellion, functional butt block	z-distance
knee height sitting	femoral epicondyle lateral, digit II	z-distance
thumbtip/fingertip reach	acromion, dactylion	Euclidian distance

While the landmarks used in these calculations varied in some cases from the points on the body used to obtain the traditional distance values, the representation of a particular human dimension remains true. The table of the mean and standard deviation values for each measurement from the two surveys appears below.

**Table 2: Mean and standard deviation values for measurements from traditional distance and extracted distance data sets. All values in mm.**

Variable	Mean Traditional	Mean Extracted	Std. Deviation Traditional	Std. Deviation Extracted
Acromion Height	585.83	577.50	37.57	37.78
Buttock-knee Length	601.55	562.99	39.48	38.44
Eye Height	779.83	776.87	45.33	47.17
Knee Height	533.95	431.85	39.79	32.01
Thumb-tip Reach	774.05	730.75	56.15	53.85

As evidenced in the table, the mean and standard deviation values for each measurement are very similar between the two data sets. The extracted data set exhibits smaller values for the mean acromion and mean eye height due to its representation of a more relaxed posturing. For the remainder of the measurements, differences in mean values can be attributed to the use of different measuring techniques and variations in the distances

described. While the mean values are similar, they can not be compared directly as measurements of the same distances. Instead, the traditional and extracted data sets define *comparable* distances. For example, the traditional buttock-knee length measurement is described as the horizontal distance from the foremost point of the kneecap to the rearmost point of the buttocks when the subject is sitting with the knees bent at right angles and the thighs parallel to each other. In the case of the extracted buttock-knee length distance measure, this value is represented by the Euclidian distance from the functional butt block point (the intersection of the center of the subject's buttocks with the seat) to the outer knee point. In this measurement, the knee point described the lateral or outer side of the knee, rather than the foremost point. Additionally, the subject was seated in a "comfortable working position," such that the knees were not necessarily bent at right angles, nor were the thighs required to be parallel to one another. It is expected that the buttock-knee length and knee height measurement values will be smaller in the extracted data set than those in the traditional data set.

### 3.2.2 Data Set Comparison

The similarity of these data sets was examined through the use of between-measurement correlations, the comparison of boundary individuals from principal components analysis, and the use of a Mantel test to determine matrix correlation.

#### *3.2.2.1 Between-Measurement Correlations*

Table 3 presents a comparison of the between-measurement correlation values for the traditional and extracted data sets. In spite of measurement differences, correlations between data measurements in the traditional distance measurement data set are markedly similar to

those of the extracted distance set, except in correlations with the buttock-knee length measurement. These similarities indicate that relationships between the measurements are preserved across the data sets.

**Table 3: Correlation table for measurements, showing values for both traditional and extracted data sets. A value of 1 indicates perfect correlation, while a value of 0 indicates no correlation between the variables.**

Variables Correlated	Traditional	Extracted
Acromion Height w/Buttock-knee Length	0.765	0.477
Acromion Height w/Eye Height	0.896	0.888
Acromion Height w/Knee Height	0.687	0.638
Acromion Height w/Thumbtip Reach	0.654	0.627
Buttock-knee Length w/Eye Height	0.810	0.449
Buttock-knee Length w/Knee Height	0.536	0.691
Buttock-knee Length w/Thumbtip Reach	0.559	0.684
Eye Height w/Knee Height	0.730	0.669
Eye Height w/Thumbtip Reach	0.690	0.675
Knee Height w/Thumbtip Reach	0.890	0.903

### 3.2.2.2 Principal Components Analysis

In order to better compare the two data sets, a principal components analysis was used to distill the five-dimensional data to a more manageable number of dimensions. Principal components analysis (PCA) is an ordination analysis method used to reduce data sets by finding orthogonal coordinate axes within the data which describe directions of maximal variation. PCA is defined in terms of correlation or covariance. When applied to distance measurements, PCA is often performed after the data has undergone log-transformation and mean-centering in order to correct for weighting of variables which contain large distance measurements over those describing smaller values [27].

After standardizing, a variance-covariance matrix is generated for the data which gives the largest weights to those variables with the largest variances. This matrix contains the covariance of each variable with the others in the off diagonals, and the variance of an individual variable on the diagonal. The matrix is generated in the following way:

$$S = \frac{1}{n-1} \sum_{i=1}^n (x_i - \mu)(x_i - \mu)^T \quad (2)$$

in which  $x$  is a vector of data for a single subject in the data set matrix,  $X$ , and  $\mu$  is a vector of the mean set of measurement values for all  $n$  subjects.

Singular-value decomposition factors the variance-covariance matrix into an eigenvector matrix,  $E$ , which describes the axes of maximum variance within the data and a diagonal matrix of singular values or eigenvalues,  $\Delta$ .

$$S = E\Delta E^T \quad (3)$$

Each eigenvector describes one of the principal components axes (a factor), and explains a percentage of the total variation within the data set. The standardized data is projected onto the principal components axes, and a reduced set of dimensions may be selected in order to summarize the data for plotting and analysis.

The results of the principal components analysis for each data set appear below in Table 4 and Table 5. These tables show the loadings for each factor, and the percentage of the total variance explained by each. The values for each loading are given in terms of correlation coefficients, with a value of 1.0 indicating a perfect correlation. In both data sets, the loading of the first principal component (factor 1) includes all mid-range, positive values of about the same magnitude. For the analysis of distance data, this factor is commonly described as a predictor of “generalized body size” as all variables increase or decrease at about the same rate [28, 29]. The values of the loadings on the first factor for each data set also demonstrate isometry, a change in size not accompanied by a change in shape. Isometry is determined for each variable relative to the first principal component as a measure of size by the allometric coefficient,  $a$ . The allometric coefficient is found for each variable by

multiplying the value of the loading by  $1/\sqrt{p}$ , where  $p$  is the number of variables. Values for  $a$  that are near 1 indicate isometry, while values greater or less than 1 indicate positive or negative allometry—changes in size accompanied by changes in shape. For both data sets, the loadings on the first factor indicate isometric growth; as subjects get larger or smaller, the relationships between their measurements remain fairly constant. Loadings of 0.4472 would indicate perfect isometry for a five-variable analysis.

**Table 4: Coefficients for the principal components from traditional distance data.**

Variable	Factor 1	Factor 2	Factor 3	Factor 4	Factor 5
Acromion Height	0.434	0.547	0.305	0.539	0.360
Buttock-Knee Length	0.422	-0.527	0.699	-0.043	-0.235
Eye Height	0.441	0.531	-0.061	-0.539	-0.479
Knee Height	0.476	-0.250	-0.275	-0.424	0.675
Thumbtip Reach	0.461	-0.283	-0.583	0.486	-0.362
Variance:	3.885	0.679	0.238	0.110	0.087
Cumulative percentage of total variance explained:	77.714	91.300	96.060	98.266	100

**Table 5: Coefficients for the principal components from extracted distance data.**

Variable	Factor 1	Factor 2	Factor 3	Factor 4	Factor 5
Acromion Height	0.437	-0.542	-0.238	0.572	-0.362
Buttock-Knee Length	0.420	0.489	-0.749	-0.147	0.035
Eye Height	0.439	-0.547	0.026	-0.618	0.355
Knee Height	0.467	0.298	0.479	-0.270	-0.625
Thumbtip Reach	0.472	0.281	0.389	0.443	0.592
Variance:	3.803	0.711	0.281	0.111	0.094
Cumulative percentage of total variance explained:	76.059	90.280	95.897	98.121	>100

The second factor for both data sets shows an inverse relationship between buttock-knee length and the variables acromion height and eye height, as the three variables have similar midrange loadings and the buttock-knee length loading is of opposite sign. These values indicate a contrast between the limb dimension (buttock-knee length) and the torso dimension descriptors (acromion height and eye height). Factors 3, 4, and 5 have been

included in the table, but will not be evaluated in the analysis. For both the traditional and extracted data, just over 90 percent of the total variation within the data set can be explained by the use of the first two factors.

The cosine of the angle between each of the principal component vectors for the two data sets was calculated in order to examine the correlation between the PCA results. For example, if the correlation between the vectors describing the first PC factor for the traditional data and the first PC factor for the extracted data is close to positive or negative one (positive or negative correlation), then this demonstrates that the vectors descriptions are nearly the same, and thus identify similar directions of variation within the data. Near-perfect correlation was found between the traditional and extracted PCA results on all factors. The correlation values for principal component vectors 1 through 5 were 0.9999, -0.9980, -0.9563, 0.9782, and -0.9446 respectively. These results confirm that the maximal directions of variation found through principal components analysis are nearly identical in the two data sets.

The plots of the first two principal components for both data sets appear in Figure 5 and Figure 6. The five-dimensional data can be visualized in this way because the first two dimensions explain most of the variation in the data sets. The x-axis represents Factor 1, generalized body size, and the y-axis represents Factor 2, a contrast between limb and torso dimensions. Subjects are differentiated on the basis of gender, denoted by '+' or 'o' in the plots. In both graphs, some separation along the first principal axis on the basis of gender is apparent. Figure 5 and Figure 6 show female subjects grouped at the low end of the x-axis, illustrating smaller body types, whereas the male subjects are grouped at the high end of the x-axis, demonstrating larger body types. Both males and females exhibit various

combinations of torso and limb length combinations, and are distributed similarly along the y-axis. Both sets of data are fairly normally distributed. In both graphs, the aspect of the x and y axes with respect to the original units of measurements has been preserved.

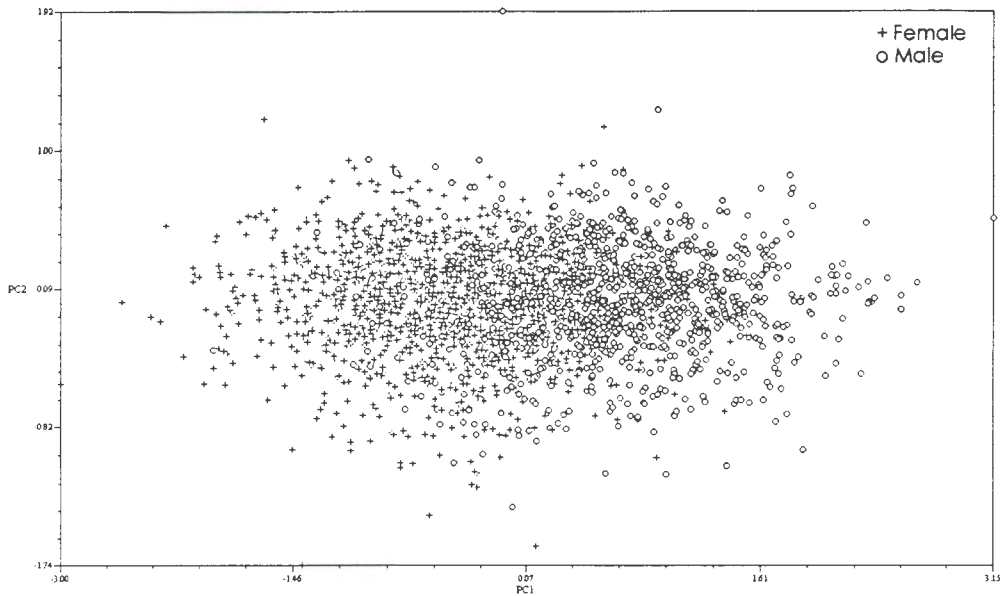


Figure 5: First two principal axes of traditional distance data.

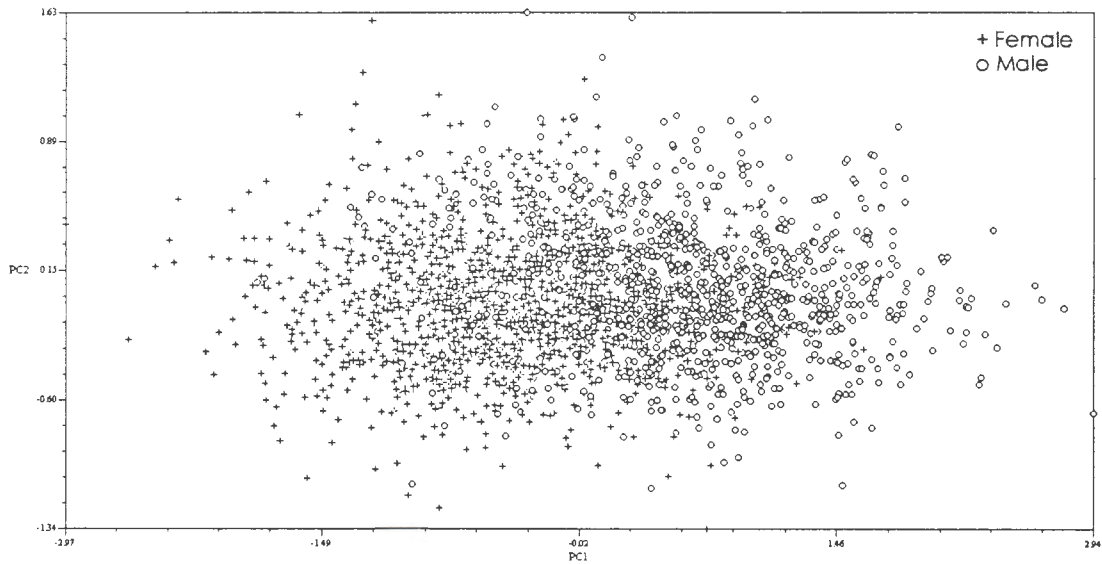


Figure 6: First two principal axes of extracted distance data.

### 3.2.2.3 Density Contours and Boundary Individuals

In keeping with the methods of multivariate workstation design, constant density contours were used to select a percentage of the population and identify boundary individuals who represent these variations by using the location of the data on the first two principal components axes. In this way, the amount of variation the contours describe is maximized.

A constant probability density contour is an ellipsoidal surface describing a constant squared distance from the mean of the data. Described in greater detail in Chapter 4, a 50<sup>th</sup> percentile density contour, for example, would encompass the 50 percent of the values statistically closest to the mean. Eight representative subjects were selected from each data set by identifying subjects nearest to the 95<sup>th</sup> percentile density contour for the first two principal components at equally spaced points along the ellipse. The 95<sup>th</sup> percentile was chosen to keep with the goal of accommodating a large percentage of the design population, and as a typical value in percentile-based design scenarios.

Those subjects closest to the extents of the ellipse on the  $x$  and  $y$  axes, as well as the intersection of the ellipse with the line  $y = \left(\frac{b}{a}\right)x$  in which  $a$  is the semi-major and  $b$  is the semi-minor axis of the ellipse were selected as the eight boundary individuals representing body-component variation within the data set. While it would be possible to recreate individuals at the exact extents of the density contour boundary, it was desirable to select the closest subject from the data set so that the individual's accompanying data (body scans, three-dimensional landmarks, and additional posturing data from the CAESAR survey) could be accessible for visualization or further analysis.

As the data has been mean centered, the equation for the density contour

$$c^2 = (x - \mu)' \Sigma^{-1} (x - \mu) \quad (4)$$

in which  $\mu$  is the multivariate mean,  $\Sigma$  is the variance-covariance matrix of the data set,  $X$ , and  $c$  is the distance to the mean reduces to

$$v = x^2 (\Sigma_{00}^{-1}) + y^2 (\Sigma_{11}^{-1}) \quad (5)$$

in which  $v$  is the chi-squared value at which the contour has been created, and  $\Sigma_{00}^{-1}$  and  $\Sigma_{11}^{-1}$  are the diagonal values of the inverted variance-covariance matrix.

Figure 7 shows the eight subjects selected from the density contour analysis of the PCA data for the traditional distance data set. Figure 8 contains the corresponding plot for the determination of cases in the extracted distance data. These graphs show the 95<sup>th</sup> percentile density contour for each data set. The dotted lines in each graph indicate the mean values on the x and y axes, and were used to select representative subjects 1, 3, 5, and 7. The diagonal lines were used to select representative subjects 2, 4, 6, and 8.

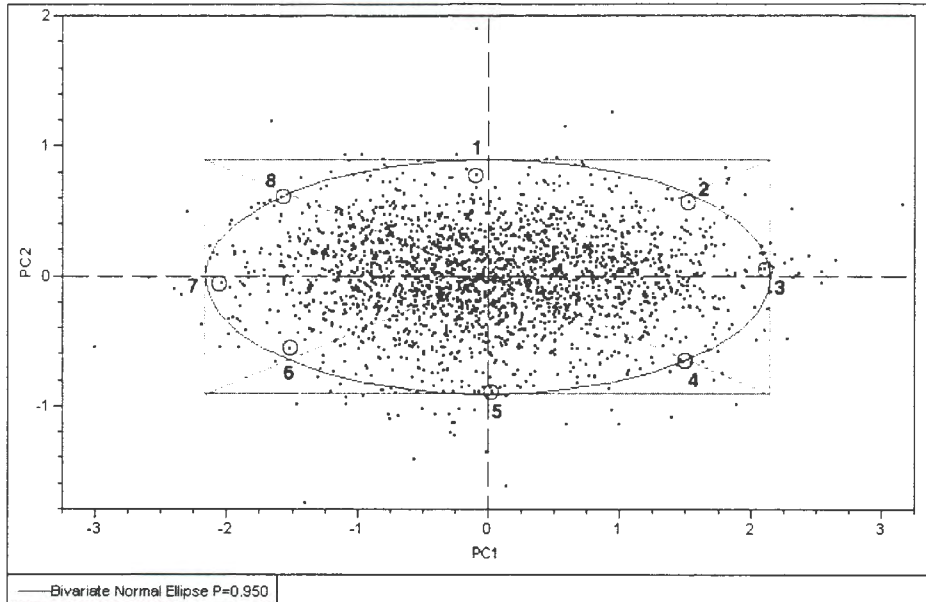
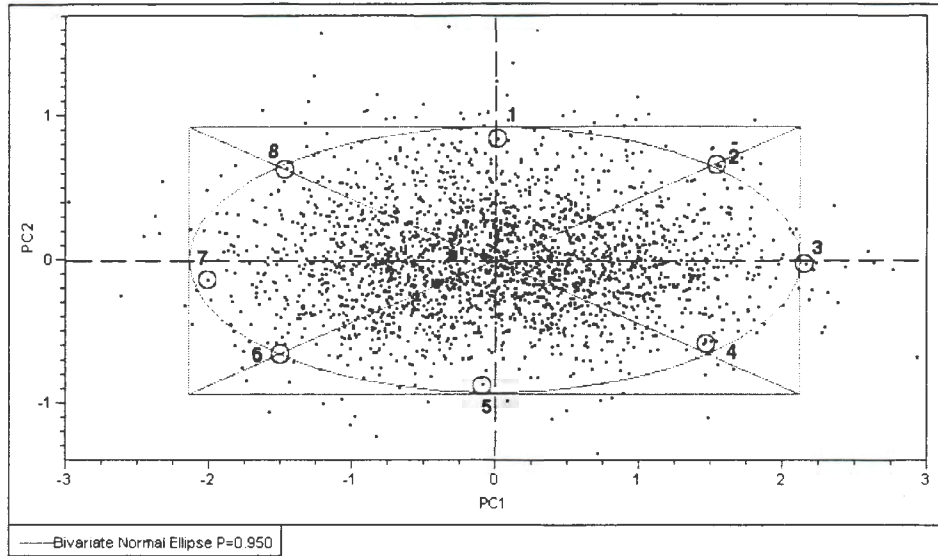


Figure 7: 95<sup>th</sup> percentile density contour and case selections for traditional distance data set.



**Figure 8: 95<sup>th</sup> percentile density contour and case selections for extracted distance data set.**

The first principal component (Factor I) displays general body size, thus the two cases at the extents of the major axis of the ellipse represent generalized small (Case 7) and generalized large (Case 3) individuals. The second principal component (Factor II) denotes the contrast between trunk and limb length measurements, thus Case 2 and Case 4 in the *traditional* data set are both large individuals, but display a contrast between trunk and limb length; Case 2 has larger trunk dimensions than Case 4, but shorter limbs. The results are similar for cases 8 and 6: both represent smaller individuals, but Case 8 has larger trunk dimensions than Case 6 but smaller limbs. Cases 1 and 5 directly contrast, with Case 1 representing an individual with larger trunk dimensions and smaller-than-average limb length and Case 5 depicting a subject with smaller trunk length and larger limb length.

As the principal components analysis for the extracted distance data yielded similar weighting in the first two factors, the results of case selection in the extracted data set are much the same. As in the analysis of the traditional data, cases 3 and 7 on the extents of the

horizontal axis (Factor I), represent the generalized large and small individual respectively. For this data, the weighting of the second principal component was reversed, so while Cases 2 and 4 are again both large individuals, Case 2 has smaller trunk dimensions than Case 4, but longer limbs. (Thus, Case 4 in the traditional data set would be most comparable to Case 2 in the extracted data set, and vice versa.) The same relationship holds between Cases 8 and 6 and Cases 1 and 5.

#### 3.2.2.4 Mantel Test of Matrix Correlation

The similarity of the two data sets was evaluated by plotting the between-subject similarity matrices against each other in a 2-way Mantel test. First, a matrix of the Euclidian distance between each of the 2307 subjects (within the five-dimensional data space) was generated for each data set—producing two, 2307x2307 matrices. These matrices were then compared element by element (ignoring the diagonal values) in order to measure their degree of correspondence through the Mantel test of significance [30]. The test evaluates degree of matrix correlation as the sum of the dot products of the off diagonal elements in the similarity matrices. If the matrices exhibit similar structure, the result is high relative to the value expected by chance. This result,  $Z$ , can also be converted into the correlation coefficient through normalization.

The results of the Mantel test showed a highly significant correlation between the similarity matrices of the PCA results from the traditional and extracted distance data sets:  $r=0.928$ . The results of this analysis indicate that the relative position of each subject within the two-dimensional, principal component data space is nearly identical. The plot for the Mantel test for correlation appears in Figure 9.

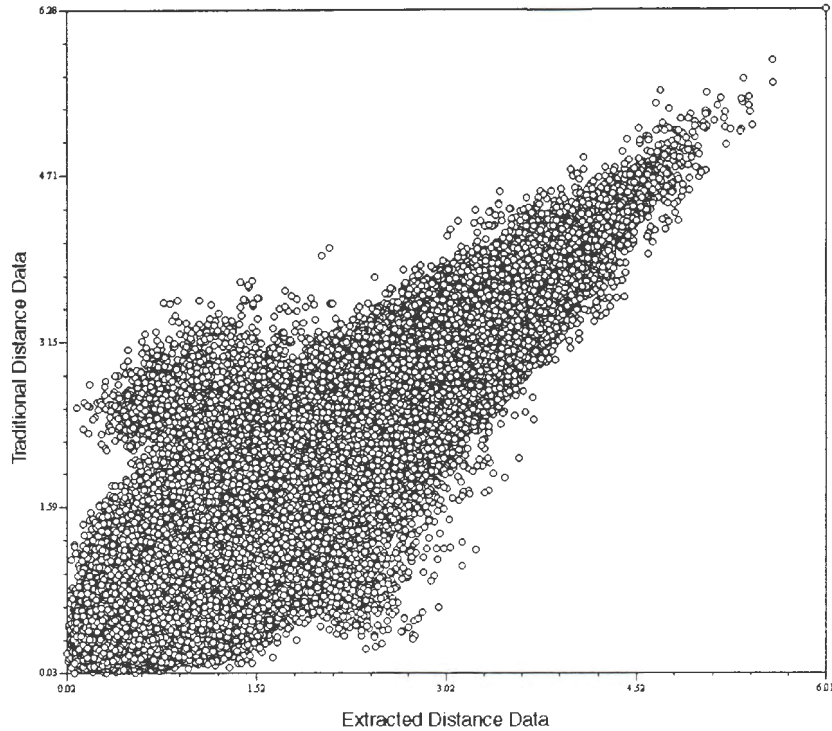


**Figure 9: Correlation plot of the results of the Mantel test including the extracted distance data and the traditional distance data sets.**

### 3.2.3 Conclusions

The results of this analysis make it clear that the inclusion of posture and the use of distance measurements extracted from a three-dimensional data set have hindered neither the analysis nor the discrimination of representative cases. A principal components analysis of the data sets found nearly identical axes of variation within the two data sets: the first PC axis represented generalized size, and the second described an inverse relationship between torso length and limb length. As a result, the two data sets yielded generalized cases representing the same design principles.

The results of the Mantel test showed significant similarity between the relative positions of the subjects within the extracted distance and traditional distance data spaces.

This means that subjects grouped closely as a result of having similar forms as described by

the traditional distance data are grouped in nearly the same way based on their description in the extracted data set.

While the traditional and extracted data sets are significantly similar and generate the same design solutions, they do so with slight differences in the dimensions they recommend. Some of the variations between the data sets (as evidenced in the differences between mean values) are a result of the use of comparable rather than identical measuring methods and descriptions. These differences stress the importance of the designer's awareness of the collection method used for each particular data set. The use of distance data requires knowledge of the relationship of the data to the physical subject. Designs based on incorrect measurement assumptions could fail to accommodate the desired population.

### **3.3 Analysis II**

#### 3.3.1 The Data

The second analysis examined the effects of higher-dimensional data on design decisions by comparing evaluations of the CAESAR population as described by both three-dimensional landmark data and extracted distance data. As the extracted distance data was calculated from the original landmark data itself, both data sets describe individuals seated in the same comfortable posture. The only difference between the data is the method of description.

As in the previous analysis, landmarks were selected in order to describe the seated dimensions of a subject for use in cockpit or workstation design. The extracted distance data set includes measures for Acromion Height, Buttock-knee Length, Eye Height Sitting, Knee Height Sitting, and Thumb-tip Reach. The landmarks used in the three-dimensional analysis

include those required to calculate the extracted distance measures: sellion, left and right acromion, left and right dactylion (tip of the middle finger), left and right femoral epicondyle lateral (outer knee), left and right digit II (tip of the second toe), and the functional butt block. As before, all data was standardized by alignment of the subject to the seat based on butt block location and the application of the extended arm positions from the standing data set to the seated data.

### 3.3.2 Data Set Comparison

The similarity of these data sets was examined through the use of principal components analysis, the evaluation of the cophenetic correlation for a dimensionally reduced representation of the complete data space, and the use of a Mantel test to determine matrix correlation

#### *3.3.2.1 Principal Components Analysis*

The methods of principal components analysis function in the same way for three-dimensional landmark data as they do for univariate distance data. In this analysis, the only difference is in the dimensionality of the data. The landmark data for each subject consists of a  $k \times p$  matrix of coordinates, in which  $k$  is the number of measurements (10 in this analysis) and  $p$  is the number of dimensions which describe the landmark location (3). The entire data set may be represented as a matrix of  $n$  rows of subjects with  $kp$  columns. Much of the methodology for analyzing landmark and distance data has been developed in the field of geometric morphometrics—methods commonly used to quantify the size and shape of anatomical objects in biological research. When analyzing three-dimensional landmark data in terms of shape, morphometric methods standardize all data with respect to size, location,

and orientation of each specimen through the alignment of all specimens to a reference (or average) shape. This standardization results in an analysis which compares shape irregardless of a subject's size, location, or orientation. The most widely used method for data alignment and standardization is called generalized Procrustes analysis (GPA) [31,32].

For the analysis of human figure data for workstation design, a different method of alignment is required. Instead of examining size-free shape, size is an important factor which must remain in the analysis. Additionally, it is the deviation from some standardized posture which concerns the designer, not necessarily deviation from the mean individual as GPA would provide. For this reason, only position and orientation are standardized in the analysis presented here. This method fits all data to a common origin in the design while maintaining the size of each individual.

Prior to standardization, the raw landmark data occupy *figure space*, the physical space in which each subject was measured. Figure space has  $pk$  dimensions, in which  $p$  is equal to the number of landmarks and  $k$  describes the dimensionality of the data. After standardization by translation and rotation, the data for each subject includes both shape and size information and occupies *form space* of  $kp - k - k(k-1)/2$  dimensions. The distribution of two-dimensional data that has undergone GPA occupies a curved space that can be visualized as the surface of a hemisphere [33]. For three-dimensional data, however, the geometry is "substantially more complicated" [34].

For the three-dimensional landmark data describing 10 landmarks, standardizing the data results in 24 dimensions of shape and size information. Thus, when the data undergoes principal components analysis, only the first 24 eigenvectors will describe shape and size variation.

In order to perform statistical analysis, the data is orthogonally projected into a linear tangent space with the consensus subject describing the point of tangency. It is this projected data which undergoes PCA, enabling the identification of directions of maximum variation within the data set. In this analysis, the factor loadings for the principal components analysis of the three-dimensional landmark data show that the first two principal components explain 52% of the variation within the data, and the first three factors explain just over 65%.

The distance-based techniques described in the previous analysis were used to perform a principal components analysis of the extracted distance data so that these results could be compared to the PCA results from the 3D landmark analysis.

Figure 10 contains the plot of the first two principal components for the 3D landmark data. Figure 11 illustrates the corresponding plot for the extracted distance data. Subjects are differentiated on the basis of gender, denoted by '+' or 'o' in the plots. In both graphs, some separation by gender along the first principal axis is apparent, although the separation is in opposite directions when the graphs are compared. In both graphs, the aspect of the x and y axes with respect to the original units of measurements has been preserved. The distribution of the data in the PCA for the 3D landmark data appears more spherical than that of the extracted data due to the percent of variation represented by each axis. The first two factors in the results of the landmark analysis represent a similar amount of variation within the data set: 31 percent and 21 percent respectively. In the case of the extracted distance data, however, the first factor represents considerably more variation than the second: 76 percent and 14 percent respectively.

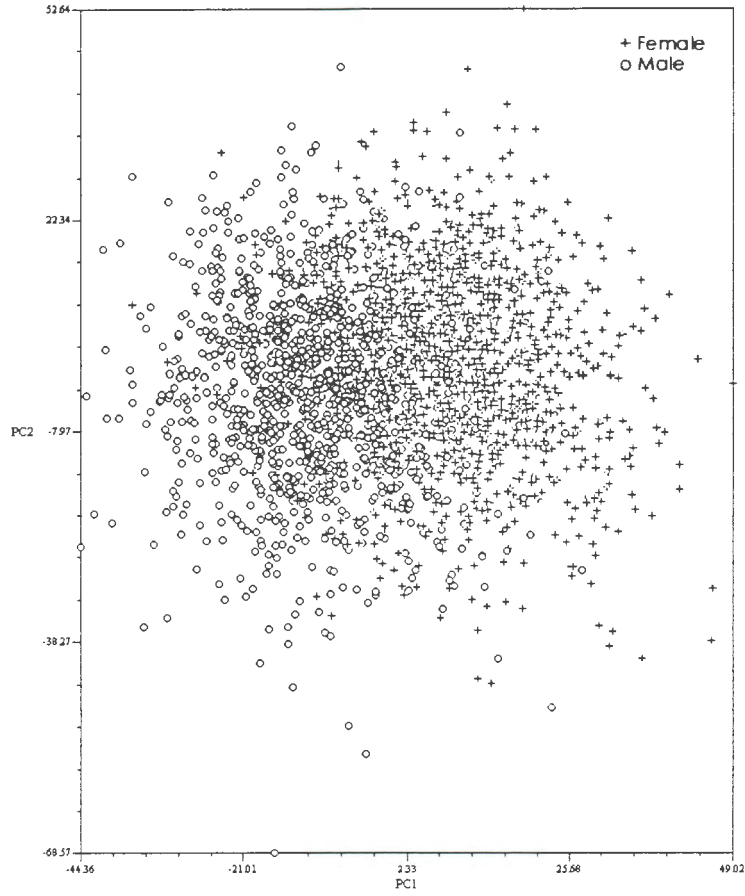


Figure 10: First two principal axes of 3D landmark data.

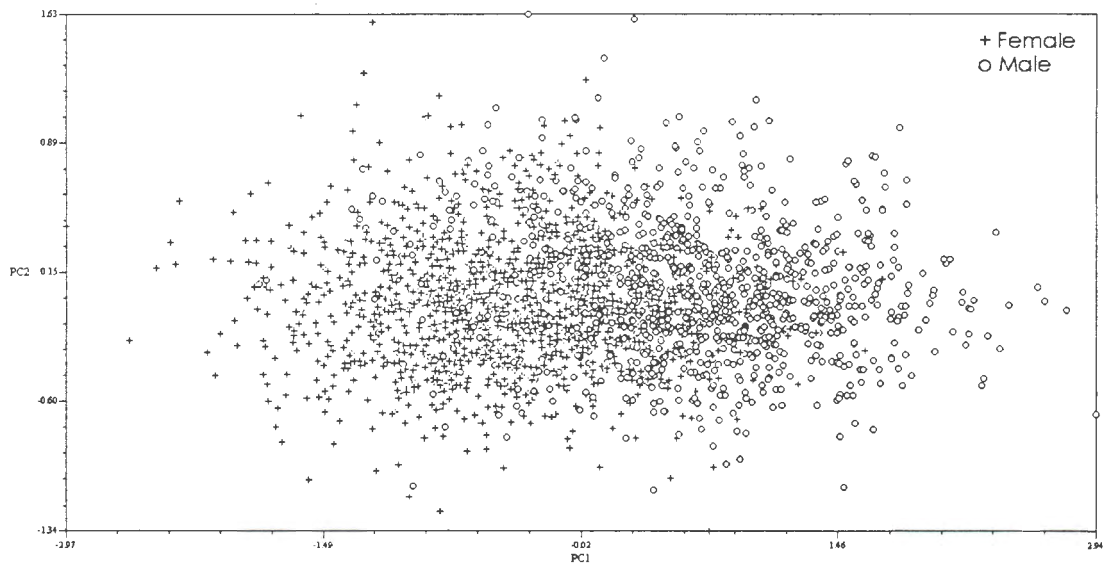


Figure 11: First two principal axes of extracted distance data.

The explanations for the first two factors from the PCA for the extracted distance data set, as delineated in Analysis I, are relatively clear. The first principal component for the extracted distance data represents generalized size, while the second denotes a contrast between limb length and torso dimensions. The results of the principal component analysis for the three-dimensional landmark data, however, are more difficult to interpret due to the high number of variables (30) and their description of x, y, or z positional values rather than direct human dimensions. Of greater import is the ability of the graph of the first two factors to accurately depict the relative locations of each subject within the data space.

### 3.3.2.2 Cophenetic Correlation

An evaluation of the ability of the first two principal components to represent the relative locations of each subject within the original, 24-dimensional form space was tested by performing a cophenetic correlation. In such an analysis, a similarity matrix for the Euclidian distances between subjects based on the dimensional analysis is compared with a similarity matrix for the Euclidian distances between objects in the complete PCA data set. If the two matrices show the same relative placements for each subject, they will produce a high cophenetic correlation, indicating low distortion [35]. For the 3D landmark data, the cophenetic correlation between the two-dimensional analysis and the twenty-four-dimensional form data suggested a mediocre fit ( $r=0.76178$ ), indicating that the 2D graph does not provide a highly accurate indication of subject's relative locations in the entire data space.<sup>i</sup> The cophenetic correlation between the first three-factors of the analysis and the full PCA data set, however, produced a correlation value indicating a good fit ( $r=0.85$ ). These

---

<sup>i</sup> Values of  $0.9 \leq r$ ,  $0.8 \leq r < 0.9$ ,  $0.7 \leq r < 0.8$ ,  $r < 0.7$  indicate a very good, good, poor, and very poor fit respectively [26].

results indicate that a plot of the first three principal components would provide a fairly accurate representation of the distribution of subjects within the entire data space. Figure 12 contains a plot of the first three principal components for the 3D landmark data analysis.

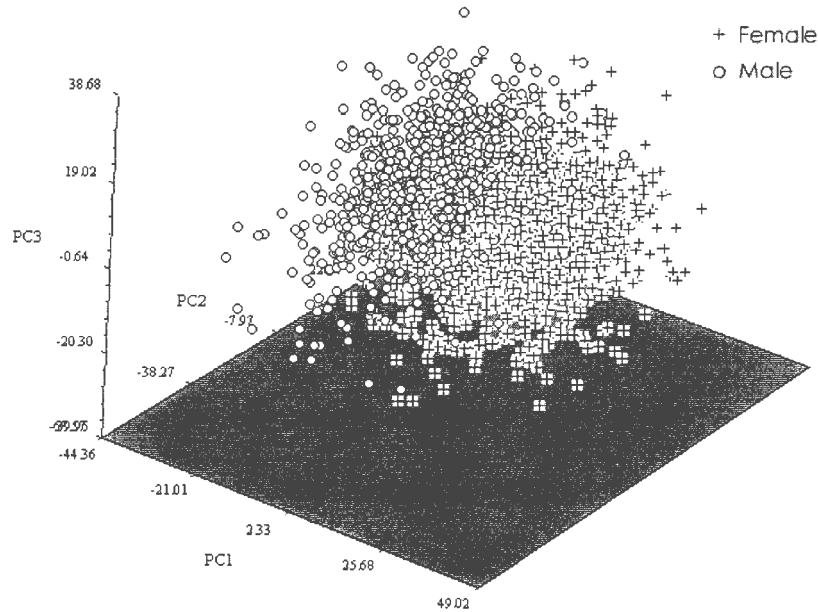


**Figure 12: The first three principal axes of the 3D landmark data.**

### 3.3.2.3 Mantel Test for Matrix Correlation

In order to investigate whether the relative positions of each subject within the PCA results from the 3D landmark and extracted distance data sets were similar, a 2-way Mantel test was performed. The results of the Mantel test showed non-significant correlation values for the between-subject Euclidian distance matrices from the first three PC axes of the extracted distance and 3D landmark data sets ( $r=0.23109$ ). When the entire set of PC axes was used to calculate distance, the correlation value from the Mantel test increased by just over  $1/100^{\text{th}}$  of a point. These results indicate that the relative positions of each subject within the data spaces of the extracted distance analysis and the 3D landmark analysis are not

similar. Figure 13 shows a graph of the correlation results. The wide spread of data points along the diagonal is indicative of a poor correlation between the data sets.

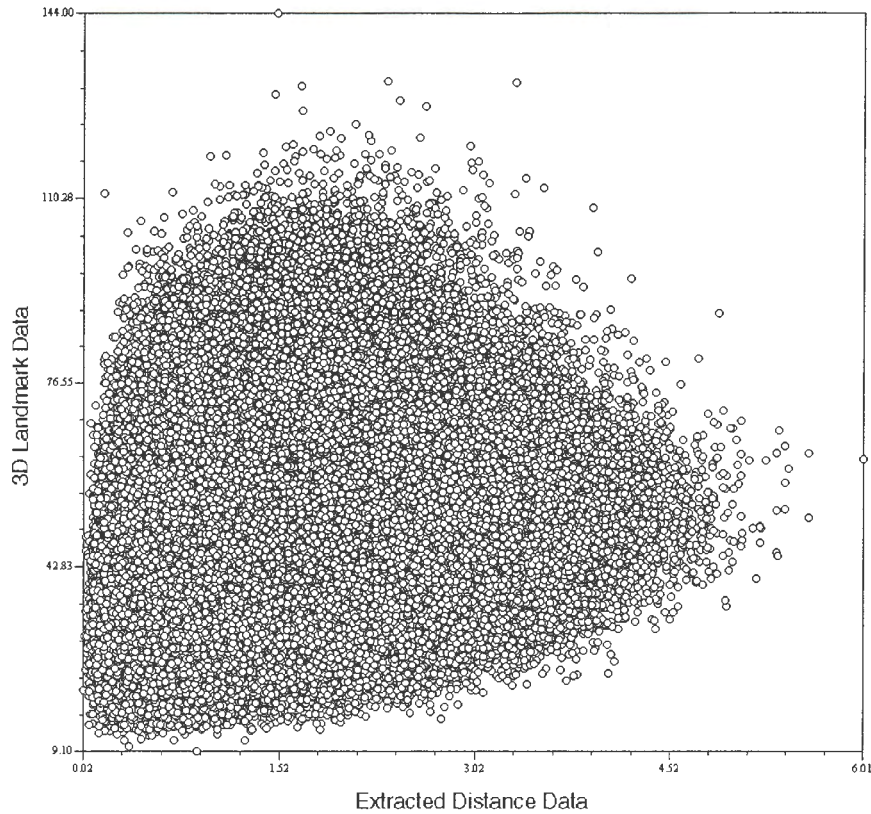


**Figure 13: Correlation results from the Mantel test involving the extracted distance data and the 3D landmark data sets.**

### 3.3.3 Conclusions

The results of this analysis stress the inability of anthropometric distance data to adequately describe the human form to the same degree that landmark data can achieve. The PCA of the distance data stressed significantly different design characteristics than did the corresponding analysis for the landmark data. The poor correlation between the 3D landmark data and the extracted distance data shows that the principal components analyses did not position subjects similarly within the data spaces. Missing in the distance analysis are descriptions of the relative positions of the limbs and torso, the posture of the subject, and the

inter-landmark relationships. The use of distance measurements over landmark data is a simplification which reduces variation within the data set, allowing for a larger amount of the variance to be explained by the first two principal components and resulting in a poor correlation between the more complete landmark data analysis.

The superiority of morphometric methods based on landmark analysis over distance-based approaches has been demonstrated by Rohlf [36,37] and accepted in the morphometrics community. For human factors and ergonomic design, it should be understood that designs built on univariate distance data fail to capture the variations in form represented by three-dimensional landmark data. Missing in univariate data are the geometric relationships and the size and shape descriptors which make landmark data a more complete archival of form. While the extracted distance data could be generalized through principal components analysis into a two-dimensional plot, a similar representation of the landmark data is an inadequate descriptor. The common design methods of using PCA and density contours to reduce the data to a 2D image in order to generate design cases is not an accurate method for this set of 3D landmark data. The 3D data set is too complex, and the variation too large to represent in the traditional, two-dimensional method.

In attempting to simplify design methods for a population, univariate methods oversimplify the description of the population and sacrifice important design information. The following chapter discusses a tool which allows designers to make use of the three-dimensional landmark data in an immersive, virtual reality environment. By viewing the data in a three-dimensional space, the variations intrinsic to an individual, the population, or a subsection of the population may be fully examined without a reduction in the order of the data. The number of landmark descriptors and the size of the subject set may be specified by

the designer. Additionally, the landmarks may be viewed either alone or in relation to computer generated models of workstation geometry, allowing for evaluation and direct comparison to a current working model.

## CHAPTER 4: WORKSTATION DESIGN TOOL

This section describes the implementation of an advanced operator workstation design tool which allows for the viewing and analysis of three-dimensional human figure data in an interactive, immersive virtual reality environment. All subsections except section 4.2.5 and 4.2.7 can be referenced to [38] with only minor changes.

The goal of the advanced operator workstation design tool is to provide designers and ergonomists with a method of accurately depicting the relationships among population data and workstation geometry. This task has been approached by developing an immersive application that enables a designer to examine these relationships in a virtual environment. Within the application, anatomical landmark data, dynamic motion paths, and whole-body surface scans of individuals and selected groups from the population database may be loaded and examined in reference to the digital workstation model.

These data sets may be viewed in true or scaled size, and can be filtered based upon their relevancy to the current design. The designer may chose to examine the population as a whole, or focus on the accommodation issues particular to a few individual representatives. Above all, this tool enables the homology of each individual to remain accessible and intact, allowing for design decisions to be made based on true human dimensions rather than composite representations built from summary statistics of one-dimensional measures.

### 4.1 Virtual Reality and Visualization

It has been well-established that the use of digital human modeling techniques can significantly diminish the cost associated with product development and prototype analysis [39]. Digital human models and virtual prototyping techniques can lessen or eliminate the

need for physical prototypes, thus decreasing the time between workstation development and validation of the design. Unlike physical mock-ups, digital prototypes can be altered quickly and reanalyzed to evaluate a design modification's impact on the overall design. Through the use of digital human modeling techniques, ergonomists and designers can vary operator characteristics as well as workstation parameters to systematically investigate functionality of a given workstation for a wide variety of users [40].

Virtual Reality moves these prototyping methods from the realm of simulation to experience. Using VR technology, designers are able to enter a computer-generated environment and interact with digital objects as they appear in real size. In the application developed as a part of this research, a hand-held wand is used to control menus, interact with the virtual objects, and navigate through the environment. A position tracking device is attached to the wand so that the three-dimensional position of the wand can be determined at any time in the application. Stereo viewing is produced through the use of synchronized shutter glasses which alternate in time with left and right eye image projections onto screens which form the walls, floor, and ceiling of the visualization environment (Figure 14).



**Figure 14: Inspection of pedal reach for a subject in a John Deere Cab using the immersive virtual environment.**

Another position tracker is attached to the user's head to track position and orientation. This tracking allows designers to move freely around the virtual space—inspecting the data from above or below, checking for interference, exploring issues of scale and fit—instead of having to spin the design environment within the plane of the screen as they would in “fishtank” or traditional desktop simulations. It is our belief that the use of immersive projection technologies and the ability to explore the design workspace in a natural three-dimensional manner gives a designer more insight into important relationships among the various environmental parameters, allowing for a more thorough, accurate, and intuitive design evaluation.

The application was developed for use in the C4 and C6 at the Virtual Reality Applications Center (VRAC) at Iowa State University and the MD Flex™ system at the John Deere Technology Center in Moline, IL. These systems are all highly immersive, synthetic environments and extensions of the CAVE™ display developed by Cruz-Neira [41]. The C4 consists of three flexible 12ft x 12ft back-projected walls and a 12ft x 12ft top-projected floor, as shown in Figure 15. Each wall has a projected resolution of 1024 x 1024 pixels. Stereoscopic images based on tracked head position are projected on each wall at 60Hz. Through the use of active stereo glasses, these images are perceived by the user to be single, fused, three-dimensional images.

The C6 is a six-sided 10ft x 10ft x 10ft room in which images are back-projected on all four walls as well as the floor and ceiling, as seen in Figure 15. As with the C4, the C6 device uses position trackers and stereo projection to create a fully immersive three-dimensional environment. The C6 images are generated by an SGI Onyx2 Infinite Reality2 Monster. The system includes six Infinite Reality graphic pipes, twenty-four 400MHz

R12000 processors, and 12 gigabytes of memory. Each graphics pipe has four 64Mbyte raster manager cards supporting the display of graphics.

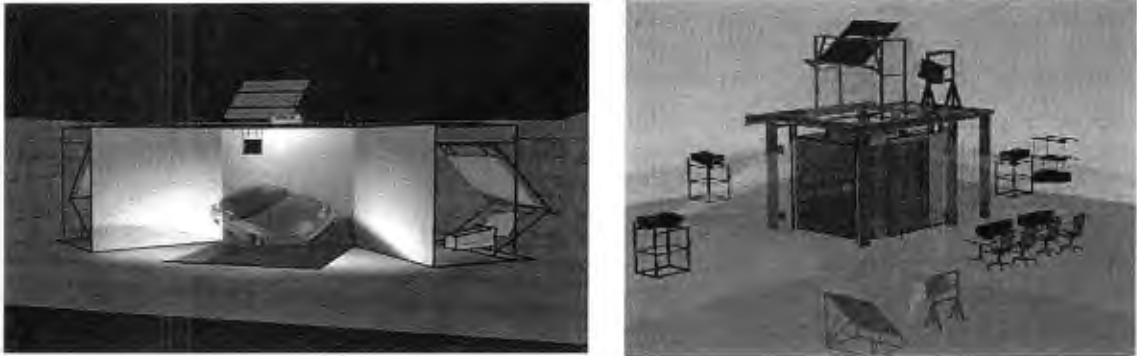


**Figure 15: The C4, image courtesy of Mechdyne Corp. (left) and the C6 (right) virtual environments.**

While the application has been primarily developed and tested in these environments, it was designed in such a way that it is easily extensible to other immersive displays. The application is based on two development tools: SGI Performer [42] and VR Juggler [43]. SGI Performer manages the scene graph, and VR Juggler is an open-source virtual reality application framework developed at VRAC which manages the multiple graphics pipes required for immersive display on multiple screens, and enables application scaling from desktop systems and head-mounted displays to Powerwall™-like and multi-screen CAVE™-like systems. I/O devices are abstracted in VR Juggler, allowing the developer to focus on the application rather than the display and device configuration.

## 4.2 Application Implementation

As an example workstation design problem, a John Deere tractor cab equipped with a John Deere seat was selected as an example of a basic, seated-operator workstation. This section describes the data processing, virtual environment interaction methods, and application functionality of the design tool.

#### 4.2.1 Processing and Viewing the Data

In order to examine the relationships among the subject data and the workstation, all data are transformed to align with the John Deere seat in the virtual environment. The butt block location was used as the common coordinate for the CAESAR data collected in the seated working posture. In order to place the CAESAR data into the John Deere seat, a relationship was developed between the location of the butt block landmark and the seat origin. The seat origin is a chair-specific landmark providing a common coordinate for the subjects sitting in the seat, and is related to the seat index point as depicted in Figure 16. The seat index point is defined by the Society of Automotive Engineers for the purposes of operator workspace design and is equivalent to the point intersection of the central vertical plane describing the centerline of a seat with the theoretical pivot axis between the human torso and thighs [44]. Upon loading data for a seated workstation design, all seated CAESAR data are aligned such that the seat origin is fixed at the origin of the virtual space and each CAESAR subject's butt block location is positioned relative to the seat origin, as shown in Figure 16. In this way, no matter what value each subject selected as a comfortable chair height, all data (including landmarks and body scans) are positioned relative to the same seated reference.

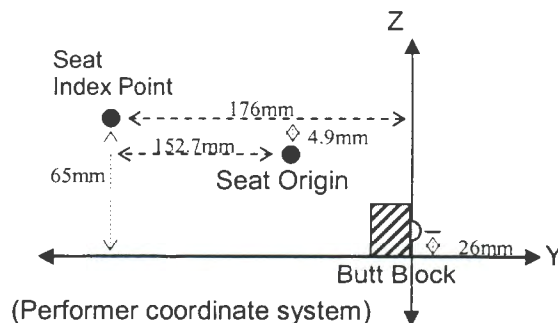


Figure 16: Relationship between seat index point, seat origin, and the CAESAR butt block landmark.

Each landmark is represented in the virtual environment as a primitive object, with different colors assigned to identify each landmark. For example, all acromion points are purple and all cervicale points are red. Distinct data sets may be designated through the use of a variety of primitive types (e.g. cubes, pyramids, and spheres). By differentiating the landmarks with color and shape, variations between data sets and landmark locations are easier to discern.

Motion path data and whole-body surface scan files are loaded into the application during startup. The motion path data was collected for an anthropometry study conducted by John Deere, and includes traces of the hand and feet for subjects performing 22 separate motions in a seated workstation environment. Figure 17 illustrates a selection of motion paths and the scan data displayed in the virtual environment. The motion path traces are text files containing vertex and polygonal data (xyz triples for vertices and the vertex indices for each face). Surface scan files are decimated and translated to the OpenFlight (FLT) file format, a standard VR file type which retains vertex color and normal information. These scans are loaded by the application after the landmark files have been loaded so that translations calculated for each subject during landmark processing can be applied to that subject's surface scan. This allows for consistent alignment of landmarks and scans in the virtual environment.



**Figure 17: Motion paths and body scan for a subject displayed in the C6.**

#### 4.2.2 Interaction Methods

Figure 18 contains an image of the RF wand, a wireless device which is used as the primary input method for this application. The wand provides access to the menuing and navigation functions, allowing the user to maneuver within the virtual space and interact with the data.



**Figure 18: The RF Wand.**

The menus consist of virtual tablets of words that can appear attached to the end of the wand in any position and orientation. The user presses buttons on the wand to cycle through menu items and select or manipulate data in the scene, as shown in Figure 19. The set of available menu commands appears in Figure 20. These commands and their use will be described in greater detail in the following sections.



Figure 19: Menu interaction in the virtual environment.

MAIN MENU	
View Menu	
Selection Menu	
Manipulation Menu	

VIEW MENU	SELECTION MENU
Change Mode display selection hide selection display only selection	Change Selection Mode add/subtract selection
Change Background Color	Set Collision Detection Modes collision on/off select landmarks or subjects
Turn Pointer On/Off	Landmark Menu (all, by type, by subject)
Landmark Menu all seated/all standing by type (e.g. head, shoulder, elbow) by subject number	Motion Path Menu (all, by type, by subject)
LineMen Menu all on/off on with collision by subject	Body Scan Menu (all, by subject)
Motion Path Menu all on/off by subject by type	Geometry Menu (all, by name)
Body Scan Menu all on/off by subject	Density Envelope Menu change density inclusion 50/90/95% all envelopes off calculate envelope by landmark type
Loaded Geometry Menu all on/off by geometry name	PCA Graph
PCA Data	

MANIPULATION MENU
Drop/Retrieve Menu
Translate Selected Geometry
Scale Selected Geometry
Turn On/Off Free-Rotate Mode
Increase/Decrease Alpha Value Of Selected

Figure 20: Commands for the Main, View, Selection, and Manipulation menus.

The user has the ability to move around virtual objects in the environment due to position and orientation tracking of the user's head. As the user walks around in the virtual environment, the views projected on the walls of the C6 and the C4 change to match the user's current position. This allows the user to look around, under, over, and between virtual objects. In order to further facilitate inspection, users also have the opportunity to reposition

the objects. When the menus are turned off, the application is in navigation mode. In this setting, navigation is button-driven. Users can maneuver around the environment and reposition the data in the virtual space to any orientation that facilitates viewing through the use of the wand.

The C4 and C6 virtual environments facilitate multiple users and collaboration within the same environment. Because the viewing perspective can only be displayed for the person with the tracked head position, other participants see a slightly distorted view of the virtual world. Finger-pointing at virtual data can often lead to confusion and misunderstanding during times when one user is communicating an idea to another user. For this reason, a virtual pointer is displayed originating from the end of the wand so that the position of the virtual pointer can be used to indicate areas of discussion. Descriptions of the data are then clear and correct for all viewers.

In the following sections, several features of the Advanced Operator Workstation Design Tool and their implementation are discussed.

#### 4.2.3 Use of Existing CAD Geometry

Workstation geometry in any of the formats supported by Performer (IGES, STL, VRML, 3DS, etc.) can be loaded into the application at startup. Each set of geometry is added as a separate entity, allowing for any translation, rotation or scaling the designer might wish to employ in order to better examine accommodation issues relevant to the data. The transparency of selected geometry may also be modified for interference or fit checking.

#### 4.2.4 Element Selection

Selection methods allow for further discrimination and inspection of the data set. Body scans may be toggled on and off so that subjects are displayed individually or as groups of scans that may be turned on to represent a composite figure. The designer may display the complete set of motion path data for a particular subject, or choose to examine all paths relevant to a particular design (e.g. comfortable above-head or seated knee-level reaches).

For landmark data, these subset selections are even more versatile. A designer may view landmark data of the whole population, or simply work with a subset of the data based on subject or landmark selection. In this way, designs dependant upon a few particular dimensions (e.g. a seated workstation dominated by the importance of shoulder fit and knee clearance) may display only a few landmark sets for particular consideration. Once representatives or “outliers” of interest in a given design situation have been determined, these representative landmarks may be highlighted. Selecting one landmark of an individual from a cluster of population landmarks activates the remainder of the landmarks corresponding to the selected individual, as shown in Figure 21. In this way, a designer may inspect large populations of users for specific fit characteristics but still consider each landmark in the data space as a full and complete individual, retrievable at any time for further examination.

Landmarks can be selected by moving the virtual pointer in contact with individual landmark primitives (collision detection) or by toggling through the selection options in the menu.

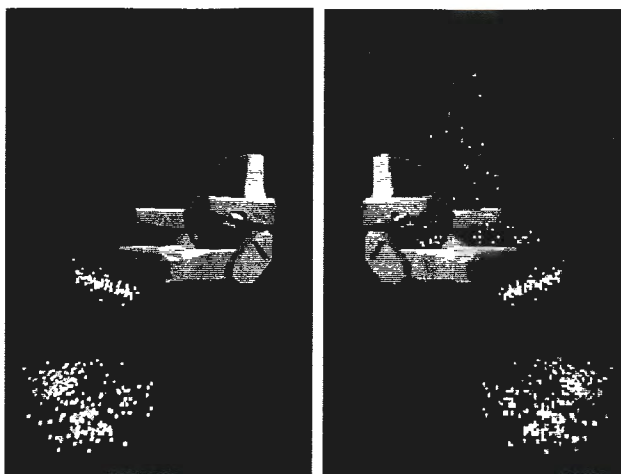


**Figure 21: (Left) Knee and foot landmarks displayed for a collection of subjects. (Right) A set of body landmarks displayed for three subjects selected from the set of knee and foot landmarks.**

#### 4.2.5 Subject Discrimination: Density Contours

The workstation design tool allows for the selection or description of a given percentage (e.g., 50 percent, 90 percent, or 95 percent) of the data for a single anthropometric landmark using density contours, as shown in Figure 22.

Constant probability density contours describe the surface of an ellipsoid for which the square of the distance,  $c$  (previously presented as Equation 4),

$$c^2 = (x - \mu)' \Sigma^{-1} (x - \mu)$$

from the mean,  $\mu$ , of a data set  $X$  (single data point  $x$ ) is constant. If  $\chi_p^2(\alpha)$  is selected as the constant, where  $\chi_p^2(\alpha)$  is the upper  $(100\alpha)$ th percentile of a chi-square distribution with  $p$  degrees of freedom, this relationship describes a solid ellipsoid of values having probability  $(1 - \alpha)$ .



Figure 22: 95th percentile density contours for individual landmarks.

A 50<sup>th</sup> percentile density contour for the sellion points of 100 individuals, for example, encompasses the 50 values statistically closest to the multivariate mean. The mean,  $\mu$ , is a three-dimensional vector containing the means of  $x$ ,  $y$ , and  $z$  coordinate values for the data set. The variance-covariance matrix,  $\Sigma$ , previously presented as Equation 2, is generated in the following way:

$$\Sigma = S = \frac{1}{n-1} \sum_{i=1}^n (x_i - \mu)(x_i - \mu)^T$$

in which  $n$  is equal to the number of subjects,  $X$  is an  $n \times p$  matrix of  $p$ -dimension observations, and  $x_i$  is a row vector from the matrix corresponding to an individual subject.

For 100 subjects represented by three-dimensional data,  $X$  would be a  $100 \times 3$  matrix. The

variance-covariance matrix is a  $p \times p$  matrix which describes the variance of each variable along the diagonal ( $s_{11} = \text{var}[x], s_{22} = \text{var}[y], s_{33} = \text{var}[z]$ ), and the covariance of each dimension variable with the others on the off-diagonals. Solving the right side of the density contour equation results in a single value—a standardized statistical distance which can be compared to the  $\chi_p^2(\alpha)$  value in which  $p = 3$  and  $\chi_p^2(\alpha)$  describes  $100(1 - \alpha)$  percent of the probability [45].

While individual density contours may prove interesting on a case-by-case design basis, perhaps of greater value is the ability to examine these statistical distance values across a set of relevant landmark points. For example, if a cab design is particularly dependant upon seated knee placement and foot reach in order to optimize fit and minimize interference, density contours may be used to explore the surfaces which encompass 90 percent of the data for each of four landmark points. As the values these contours generate are standardized distance measures, they may be compared between landmark types without any additional calculations.

Designers interested in examining the 90 percent of the subjects who are closest to the mean of each of these landmarks, can use the values generated from the individual landmark contours to do so. By summing these four distances for each subject (distance from mean for left knee + distance from mean for right knee + ...), subjects may be ranked based on this summed value and the 90 percent with the smallest summation total may be selected. These would be the subjects with the overall least deviation from the landmark means. As the statistical distances describe *relative* distance rather than true, Euclidean distances, designers can be sure that no set of distance values for a particular landmark will skew the results—

even if the deviation of those landmark points is far greater than that for any of the other landmarks.

Using this method has unique design implications. After standardizing the entire data set for position, density contours may be used to examine variation relevant to individual size and shape variations while including the effects of comfortable posturing on landmark position.

#### 4.2.6 Posture Data Examination Methods

While traditional anthropometry methods sought to standardize human figure data through the use of erect posturing, the landmark and scan data collected through the CAESAR project were obtained from individuals in comfortable seated or standing positions, enabling the capture of more realistic posturing. Although allowing free expression of comfortable or real working posture introduces variability into an analysis of human 3D anthropometry, this variability contains important design information relevant to meaningful expressions of individual differences. In the traditional approach of using a standardized erect posture and describing the 3D human form as a collection of one-dimensional measures, the important “individual differences” design information is lost.

When visualizing point-clouds of landmark data in the virtual environment, posturing of an individual subject is not easy to discern, and harder still to compare against the data set as a whole. The advanced workstation design tool enables a designer to view these relationships in the form of “LineMen.” These LineMen are similar to the line and point style skeletons used in kinematic techniques, but instead of connecting internal joint centers, LineMen represent relationships between landmark locations. Connective lines may be

specified by the designer so that particular postures may be examined in detail, as seen in Figure 23.

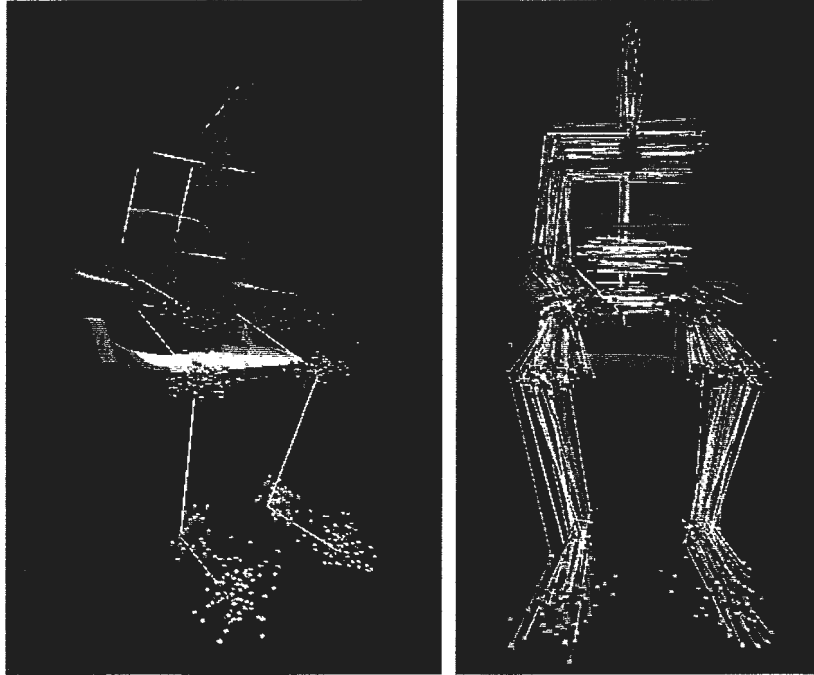


**Figure 23: (Left) LineMan displayed from an individual selected from a population of landmark data. (Right) LineMen for a population displayed with their landmark data.**

These LineMen describe the extents of each individual by connecting surface locations, and give insight into a particular posturing element. LineMen allow the designer to examine these posturing differences without having to deal with occlusion or overlap issues introduced by exploring the same data directly from a surface scan. In addition to revealing posture, the LineMen allow greater visibility of the individual within the population, and can also be drawn when the designer would like to examine all data corresponding to a particular subject.

#### 4.2.7 Principal Components Analysis

In order to discriminate subjects on the basis of form, the principal component analysis methods described in Section 3.3 are available as a means of selection in the virtual environment. PCA is performed on all complete landmark data during startup of the application. The landmarks used in the analysis (e.g., the 10 landmarks included in Analysis II) may be specified to fit the design criterion. The principal components analysis results in the reduction of the data into a three-dimensional plot which identifies the major directions of variation within the data set. Each subject is represented as a point within these first three principal component axes, found in Section 3.3 to be a fairly accurate representation of the relative locations of each subject within the entire form space.

Figure 24 shows the principal components plot displayed in the virtual environment. In this figure, two subjects have been selected from the plot, and their corresponding landmarks have been highlighted with a LineMan and identification at the sellion landmark. The three-dimensional principal components graph is displayed in the virtual environment with each axis labeled, and may be selected, repositioned, scaled or rotated in the virtual environment in order to facilitate use.

This plot enables three-dimensional exploration of a multidimensional design discrimination problem. Individual subjects may be selected from the PCA plot, causing their corresponding landmarks to be highlighted and identified in the design space. In this way, the user is able to interactively explore of the major axes of variation in form for the loaded population, examining outliers or interpreting the results of the principal components analysis in an intuitive way.

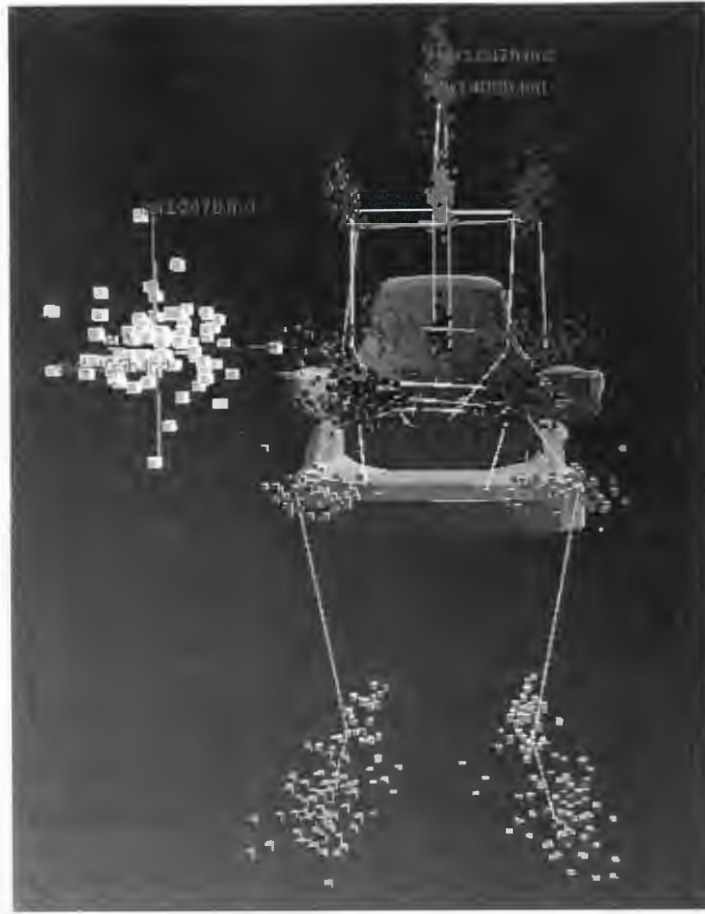


**Figure 24:** Two subjects selected from the principal components plot for the displayed landmark data.

## CHAPTER 5: CONCLUSIONS

### 5.1 Conclusions and Discussion

In the first analysis, the Mantel test comparing traditional and extracted distance data yielded a highly significant correlation between the two data sets, establishing the use of extracted, posture-inclusive data as a comparable design solution. When the extracted distance data was compared to the 3D landmark set from which it originated, however, the results were highly uncorrelated. The results of this analysis demonstrate the degree to which distance-based data sets over-simplify the description of the human form by failing to provide descriptions of the relative positions of the limbs and torso, the posture of the subject, and the inter-landmark relationships. The use of physical distances in analyses of form and shape has been almost completely replaced by landmark analysis methods in the field of morphometrics [46]. Biologists and morphometricians have recognized the inadequacy of distance data to represent the shape of the original form and as a means to investigate shape variation.

A closer approximation to the overall description of form afforded by the use of landmark coordinates might be obtained in an analysis involving distances if the body were described using the truss method (Figure 25). A truss is a collection of inter-landmark distances which attempt to exhaustively measure body form by joining four neighboring measurement points in all possible directions [47]. Even this method is an incomplete description, and only an attempt to express the geometric relationships between key locations which could be best described using landmark coordinates.

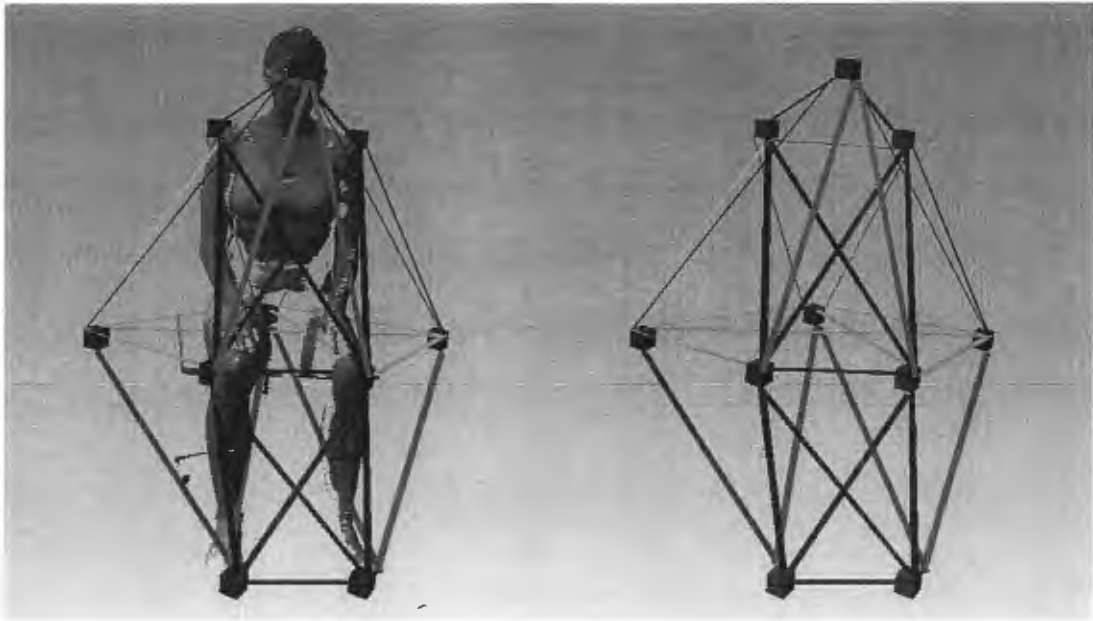


**Figure 25: A possible truss configuration for the analysis based on 10 landmarks. Thirty-two connective distances are shown.**

It is possible to distill the variation within the collection of 2307 CAESAR subjects utilized in this survey into eight generalized cases of five distance measures, but this does not mean that that these representations would provide an accurate or effective design solution. While the use of cases, percentile based look-up tables and general descriptions using distance data ease accommodation procedures for the designer, this does not mean that they should be the only guidelines for design.

Descriptions of the human form can be more accurately expressed with three-dimensional data. With the increasing availability of three-dimensional data sets, designers must begin to incorporate these new descriptors by developing tools and methods which simplify their use while taking full advantage of their richness.

Virtual reality is an ideal medium in which to explore this three-dimensional data. The workstation design tool described in Chapter 4 provides designers with the ability to view an entire population of users in relation to a workstation layout and examine

relationships that exist among the data and CAD models of workstation prototypes. A designer may examine individual subjects, a subset of the population, specific landmark configurations, or the entire data set in an immersive environment. Through the use of stereo projection, interactive menus, and the ability to load workstation geometry and CAD models, this tool makes descriptive, 3D figure information available in an intuitive design setting. Through the combination of three-dimensional data and an immersive viewing environment, design decisions can be made based on true population data and selected individuals rather than on summary statistics and composite humans.

## **5.2 Recommendations for Future Work**

The immersive advanced operator workstation design tool could be advanced in a variety of ways which would provide additional functionality or alternate design methods. The application is currently a third-person viewer; the designer moves around the environment as an observer rather than an active participant. Future versions of the application could allow the user to assume a first-person role by constraining the view of the virtual environment to a particular data subject's viewing location rather than the location of the tracked glasses. In this way, for example, users would be able to experience the seated eye height of a 6' man, or the visibility limitations of a 4'8" woman. In first-person mode, only the horizontal and vertical head positioning would be constrained; the user would be free to examine the environment by rotating within the virtual space.

Demographic data could be utilized as an optional filtering method so that designers may target specific age ranges, ethnic backgrounds, gender, or other distinguishing

characteristics as design criteria. Demographic data are currently available for all CAESAR subjects.

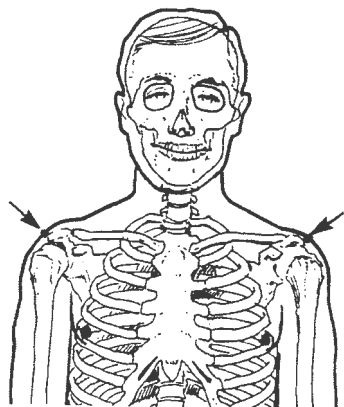
In addition to modifications to the application, future work could focus on expansion of the 3D anthropometry data set. The CAESAR data is an excellent beginning, but there were some design elements not collected in this survey. Future data collections could include the scanning of subjects in seated environments that incorporate back support. With appropriately placed cut-outs to enable the recording of posterior spinal landmarks, complete seated posture data could be obtained that would have high value to seated operator design. Additionally, the collection of motion path and reach envelope data during scanning or other anthropometric surveys would enable designers to examine control accessibility and derive joint centers based on the tracked kinematics.

## APPENDIX

### A. Three-Dimensional Landmark Descriptions

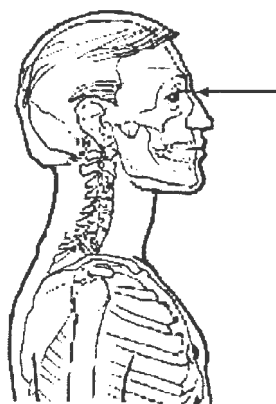
Landmark Name: Acromion, Left and Right

Most lateral point of the lateral edge of the acromial process of the scapula.



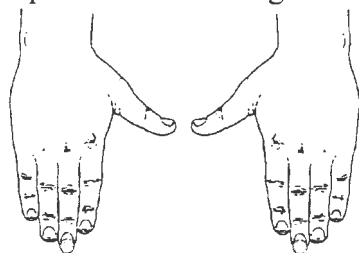
Landmark Name: Sellion

Point of greatest indentation of the nasal root depression.



Landmark Name: Dactylion, Left and Right

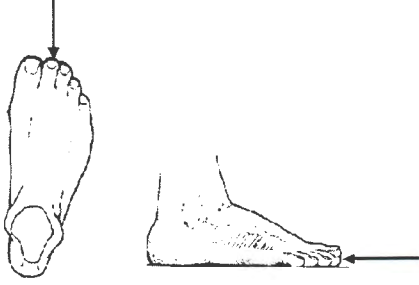
Tip of the middle finger.



Landmark Name: Digit II, Left and Right

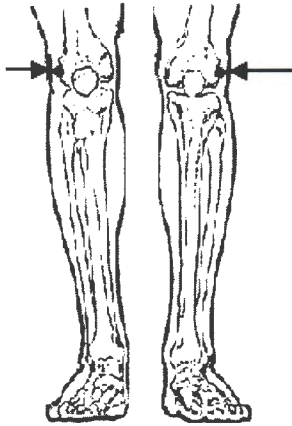
Tip of the second toe.

Note: for scans, the adhesive dot marking landmark location was placed on the tip of the toe, not on the toenail.



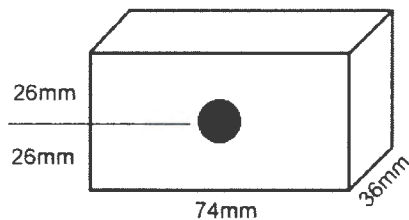
Landmark Name: Femoral Epicondyle, Lateral; Left and Right  
Lateral point on the lateral epicondyle of the femur.

Note: landmark location marked while the subject was standing.



Landmark Name: Butt Block

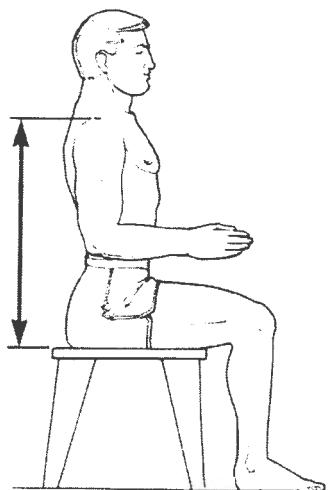
The butt block landmark is described with the placement of a small wooden block placed behind the seated subject on the flat seat surface, in light contact with the subject's buttocks.



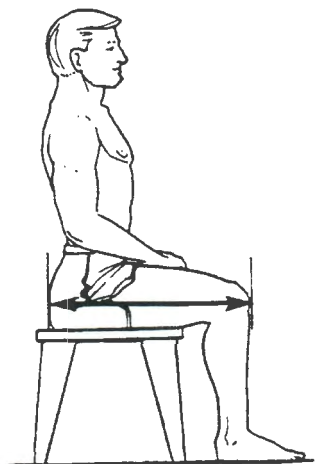
## B. Traditional Distance Descriptions

All seated distances were measured while subject was seated erect on a flat surface, knees bent at right angles, thighs parallel to each other and feet in line with the thighs. Upper arms hang down freely and forearms are horizontal.

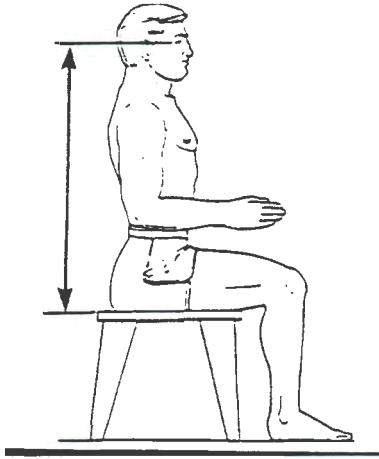
Dimension Name: Acromion Height, Sitting  
Vertical distance from a horizontal sitting surface to acromion.



Dimension Name: Buttock-Knee Length  
Horizontal distance from the foremost point of the kneecap to the rearmost part of the buttock.

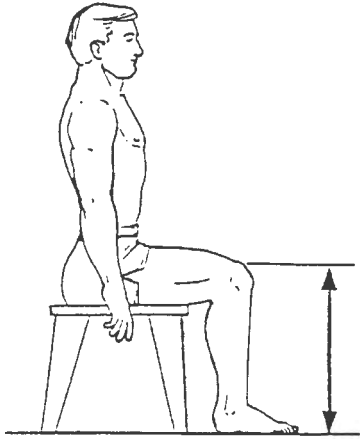


Dimension Name: Eye Height, Sitting  
Vertical distance from a horizontal sitting surface to the outer corner of the eye.



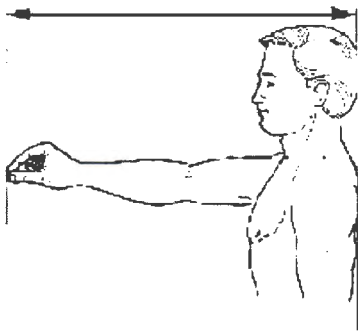
Dimension Name: Knee Height

Vertical distance from the floor or foot support surface to the highest point of the border of the patella.



Dimension Name: Thumb Tip Reach

Maximum horizontal reach measured from the back (wall surface) to the juncture of the index finger and thumb.



## REFERENCES

- [1] Robinette, K., Blackwell, S., Daanen, H., Fleming, Boehmer, M., Brill, T., Hoeflerlin, D., and Burnsides, D. (2002). *Civilian American and European Surface Anthropometry Resource (CAESAR), Final Report, Volume I: Summary*. AFRL-HE-WP-TR-2002-0169, United States Air Force Research Laboratory, Human Effectiveness Directorate, Crew System Interface Division. 2255 H Street, Wright-Patterson AFB OH 45433-7022.
- [2] Blackwell, S., Robinette, K., Daanen, H., Boehmer, M., Fleming, S., Kelly, S., Brill, T., Hoeflerlin, D., and Burnsides, D. (2002). *Civilian American and European Surface Anthropometry Resource (CAESAR), Final Report, Volume II: Descriptions*. AFRL-HE-WP-TR-2002-0173, United States Air Force Research Laboratory, Human Effectiveness Directorate, Crew System Interface Division. 2255 H Street, Wright-Patterson AFB OH 45433-7022.
- [3] *Man-Systems Integration Standards, Revision B*. (1995). Man-Systems Integration Standards. Technical document NASA-STD-3000. <http://msis.jsc.nasa.gov/>. Date retrieved: January 18, 2003.
- [4] Military Handbook: Anthropometry of U.S. Military Personnel. Department of Defense Document No. DOD-HDBK-743A. Released February 13, 1991.
- [5] Churchill, E., Churchill, T., McConville, J.T., and White, R.M. (1977). *Anthropometry of Women of the U.S. Army—1977, Report No. 2 – The Basic Univariate Statistics*. Technical report NATICK/TR-77/024, U.S. Army Natick Research and Development Command, Natick, MA.
- [6] Clauser, C.E., Tucker, P., McConville, J.T., Churchill, E., Laubach, L.L., Reardon, J. (1972). *Anthropometry of Air Force Women*. Technical report ARML-TR-70-5, Aerospace Medical Research Laboratory, Wright-Patterson Air Force Base, Ohio.
- [7] Churchill, E., Churchill, T., Kikta, P. (1977). *The AMRL Anthropometric Data Bank Library: Volumes I-V*. Technical report AMRL-TR-77-1, Aerospace Medical Research Laboratory, Wright-Patterson Air Force Base, Ohio.
- [8] O'Brien, R. and W.C. Shelton. (1941). *Women's Measurement for Garment and Pattern Construction*. U.S. Dept. of Agriculture, Miscellaneous Publication No. 454, U.S. Government Printing Office, Washington D.C.
- [9] Anonymous. (1994). Plan and Operation of the Third National Health and Nutrition Examination Survey, 1988-94. National Center for Health Statistics. Vital Health Stat 1(32) 1994.
- [10] Stoudt, H.W., Damon, A., McFarland, R., and Roberts, J. (1965). *Weight, Height, and Selected Body Dimensions of Adults, United States, 1960-1962*. Public Health Service

Publication No. 1000, Series 11, No. 8, U.S. Government Printing Office, Washington D.C.

- [11] *Multivariate Analysis*. Computerized Anthropometric Research and Design Laboratories. <http://www.hec.afrl.af.mil/cardlab/applications/multivariate.html>. Date retrieved: September, 2002.
- [12] *Jack*. Electronic Data Systems. <http://www.plmsolutions-eds.com/products/efactory/jack/>. Date retrieved: May 2002.
- [13] *Safework, Human Modeling Technology*. Dassault Systems. <http://www.safework.com>. Date retrieved: May 2002.
- [14] *Ergonomics and Simulation*. Human Solutions. [http://www.human-solutions.com/main\\_produkte\\_ergo\\_e.php](http://www.human-solutions.com/main_produkte_ergo_e.php). Date retrieved: April 2003.
- [15] *Human Simulation*. Boston Dynamics. <http://www.bdi.com>. Date retrieved: May 2002.
- [16] K.M. Robinette, WPAFB, USA, H. Daanen, TNO, The Netherlands, E.Paquet, NRC, Canada. (1999). *The CAESAR Project: A 3-D Surface Anthropometry Survey*. National Conference on Health Statistics, Washington D.C., August 1999
- [17] Gordon, C.C., Churchill, T., Clauser, C.E., Bradtmiller, B., McConville, J.T., Tebbetts, I., and Walker, R.A. (1989). *1988 Anthropometric Survey of U.S. Army Personnel: Summary Statistics Interim Report*. Natick TR-89/027. Natick, MA: U.S. Army Natick Research, Development and Engineering Center.
- [18] Robinette, K.M., and McConville, J.T. (1981). *An Alternative to Percentile Models*. SAE Technical Paper 810217. Warrendale, PA: Society of Automotive Engineers.
- [19] Bittner, A.C., Jr. (1974). *Reduction In User Population As The Result Of Imposed Anthropometric Limits: Monte Carlo Estimation*. (TP-74-6). Point Mugu, CA: Naval Missile Center.
- [20] Devore, J.L. (2000). *Probability and Statistics for Engineering and the Sciences*, Pacific Grove, CA: Duxbury Press. Chapters 12 and 13.
- [21] Meindl, R., Hudson, J., Zehner, G. (1993). *A Multivariate Anthropometric Method for Crew Station Design*. AL-tr-1993-0054. Wright-Patterson Air Force Base, OH: Crew Systems Directorate, Human Engineering Division.
- [22] Bittner, A., Wherry, R., and Glenn, F. (1986). *CADRE: A Family of Manikins for Workstation Design*. Technical Report 2100.07B. Warminster, PA: Man-Machine Integration Center, Naval Air Development Center.
- [23] Rohlf, F.J., Marcus, L.F. (1993). *A Revolution in Morphometrics*. Trends in Ecology and Evolution, Vol. 8, No. 4, April 1993.

- [24] Alexander, T., Conradi, J. (2001). *Analysis of Anthropometry and Range Validity of the Digital Human Model RAMSIS*. Technical Paper No. 2001-01-2104. Warrendale, PA: Society of Automotive Engineers, Inc.
- [25] SAS Institute. (2002). *JMP User's Guide, Version 5*. SAS Institute, Cary, N.C.
- [26] Rohlf, F.J. (2000). *NTSYS-pc: Numerical Taxonomy and Multivariate Analysis System, Version 2.1, User Guide*. Exeter Software, New York.
- [27] Darroch, J.N., Mosimann, J.E. (1985). *Canonical and principal components of shape*. *Biometrika*. 72:241-252.
- [28] Jolicoeur, P. (1963). *The multivariate generalization of the allometry equation*. *Biometrics*. 19:497-499.
- [29] Bookstein, F.L., B. Chernoff, R.L. Elder, J.M. Humphries, C.R. Smith, and R.E. Strauss. (1985). *Morphometrics in evolutionary biology*. Academy of Natural Sciences, Philadelphia, PA.
- [30] Mantel, N.A. (1967). *The detection of disease clustering and a generalized regression approach*. *Cancer Res*. 27: 209-220.
- [31] Gower, J.C. (1975). *Generalized Procrustes analysis*. *Psychometrika*, 40: 33-51.
- [32] Rohlf, F.J., Slice, D. (1990). *Extensions of the Procrustes method for the optimal superimposition of landmarks*. *Systematic Zoology*, 39:40-59.
- [33] Rohlf, F.J. (1996). *Morphometric spaces, shape components and the effects of linear transformations*. *Advances in Morphometrics*, Ed. L.F. Marcus et al. New York: Plenum Press.
- [34] Goodall, C.R. (1992). *Shape and image analysis for industry and medicine*. Short course, XIIth Leeds workshop. University of Leeds, Leeds, UK.
- [35] Rohlf, F.J. (1972). *An empirical comparison of three ordination techniques in numerical taxonomy*. *Systematic Zoology*. 21:271-280.
- [36] Rohlf, F.J. (2000). *On the use of shape spaces to compare morphometric methods*. *Hystrix Int. J. Mamm.* 11, 8-24.
- [37] Rohlf, F.J. (2000). *Statistical power comparisons among alternative morphometric methods*. *American Journal of Phys. Anthropology*. 111, 463-478.
- [38] Cerney, M.M., Duncan, J.R., Vance, J.M. (2002). *Using Population Data and Immersive Virtual Reality for Ergonomic Design Of Operator Workstations*. Presented at SAE Digital Human Modeling Conference, Munich, Germany, June 2002.
- [39] Brown, Alan S. (1999). *Role Models: Virtual People Take On the Job of Testing Complex Designs*. *Mechanical Engineering*. p. 44.

- [40] Bowman.(2001). *Using Digital Human Modeling in a Virtual Heavy Vehicle Development Environment*. Digital Human Modeling for Vehicle and Workplace Design. Chaffin, D.B., Nelson, C., Ianni, J.D., Punte, P.A.J. (eds.) Society of Automotive Engineers, March 2001, pp. 77 - 100.
- [41] Cruz-Neira, C., Sandin, D.J., DeFanti, T.A. (1993). *Surround-screen Projection-based Virtual Reality: The Design and Implementation of the CAVE*. Proceedings of SIGGRAPH 1993. pp. 135-142.
- [42] *OpenGL Performer*. Silicon Graphics, Inc. <http://www.sgi.com/software/performer/>. Date retrieved: April 2003.
- [43] *VR Juggler – Open Source Virtual Reality Tools*. VR Juggler. <http://www.vrjuggler.org>. Date retrieved: April 2003.
- [44] *Determining Seat Index Point*. Society of Automotive Engineers Standard. Document No: J1163. August 1997.
- [45] Johnson, R.A., Wichern, D.W. *Applied Multivariate Statistical Analysis*. Upper Saddle River, NJ: Prentice Hall. Fourth Edition, 1993.
- [46] Bookstein, F.L. (1991). *Morphometric Tools for Landmark Data*. NY: Cambridge University Press.
- [47] Strauss, R.E., Bookstein, F.L. (1982). *The truss: body form reconstruction in morphometrics*. *Systematic Zoology*. 31(2):113-135.